

Aus der Klinik für Neurologie
(Prof. Dr. med. M. Bähr)
der Medizinischen Fakultät der Universität Göttingen

**Extracellular vesicles derived from neural
progenitor cells stimulate
neuroregeneration in a rodent stroke
model**

INAUGURAL-DISSERTATION

zur Erlangung des Doktorgrades
der Medizinischen Fakultät der
Georg-August-Universität zu Göttingen

vorgelegt von

Xuan Zheng

aus

Guangzhou, China

Göttingen 2021

Dekan: Prof. Dr. med. W. Brück

Betreuungsausschuss

Betreuer/in: Prof. Dr. med. T. R. Döppner

Ko-Betreuer/in: Prof. Dr. med. G. Wulf

Prüfungskommission

Referent/in:

Ko-Referent/in:

Drittreferent/in:

Datum der mündlichen Prüfung:

Hiermit erkläre ich, die Dissertation mit dem Titel "Extracellular vesicles derived from neural progenitor cells stimulate neuroregeneration in a rodent stroke model" eigenständig angefertigt und keine anderen als die von mir angegebenen Quellen und Hilfsmittel verwendet zu haben.

Göttingen, den
.....
(Unterschrift)

List of publications obtained during the doctoral thesis period

Publications as first author

Publication 1: Zheng X, Zhang L, Kuang Y, Venkataramani V, Jin F, Hein K, Zafeiriou MP, Lenz C, Moebius W, Kilic E, et al. (2021b): Extracellular Vesicles Derived from Neural Progenitor Cells--a Preclinical Evaluation for Stroke Treatment in Mice. *Transl Stroke Res* 12, 185-203

Publication 2: Zheng X, Bahr M, Doeppner TR (2019): From Tumor Metastasis towards Cerebral Ischemia-Extracellular Vesicles as a General Concept of Intercellular Communication Processes. *Int J Mol Sci* 20(23):5995.

Publication 3: Zheng X, Hermann DM, Bahr M, Doeppner TR (2021a): The role of small extracellular vesicles in cerebral and myocardial ischemia-Molecular signals, treatment targets, and future clinical translation. *Stem Cells* (in press).

Publication as first co-author

Publication 4: Haupt M, Zheng X, Kuang Y, Lieschke S, Janssen L, Bosche B, Jin F, Hein K, Kilic E, Venkataramani V, et al. (2020a): Lithium modulates miR-1906 levels of mesenchymal stem cell-derived extracellular vesicles contributing to poststroke neuroprotection by toll-like receptor 4 regulation. *Stem Cells Transl Med* (in press)

Other publications

Publication 5: Kuang Y, Zheng X, Zhang L, Ai X, Venkataramani V, Kilic E, Hermann DM, Majid A, Bahr M, Doeppner TR (2020): Adipose-derived mesenchymal stem cells reduce autophagy in stroke mice by extracellular vesicle transfer of miR-25. *J Extracell Vesicles* 10, e12024

Publication 6: Haupt M, Zechmeister B, Bosche B, Lieschke S, Zheng X, Zhang L, Venkataramani V, Jin F, Hein K, Weber MS, et al. (2020b): Lithium enhances post-stroke blood-brain barrier integrity, activates the MAPK/ERK1/2 pathway and alters immune cell migration in mice. *Neuropharmacology* 181, 108357

Publication 7: Lieschke S, Zechmeister B, Haupt M, Zheng X, Jin F, Hein K, Weber MS, Hermann DM, Bahr M, Kilic E, et al. (2019): CCL11 Differentially Affects Post-Stroke Brain Injury and Neuroregeneration in Mice Depending on Age. *Cells* 9

Publication 8: Zhang L, Graf I, Kuang Y, Zheng X, Haupt M, Majid A, Kilic E, Hermann DM, Psychogios MN, Weber MS, et al. (2020): Neural Progenitor Cell-Derived Extracellular Vesicles Enhance Blood-Brain Barrier Integrity by NF-kappaB (Nuclear Factor-kappaB)

Dependent Regulation of ABCB1 (ATP-Binding Cassette Transporter B1) in Stroke Mice. *Arterioscler Thromb Vasc Biol*, ATVBAHA120315031

Publication 9: Doeppner TR, Zechmeister B, Kaltwasser B, Jin F, **Zheng X**, Majid A, Venkataramani V, Bahr M, Hermann DM (2018): Very Delayed Remote Ischemic Post-conditioning Induces Sustained Neurological Recovery by Mechanisms Involving Enhanced Angiogenesis and Peripheral Immunosuppression Reversal. *Front Cell Neurosci* 12, 383

The following thesis comprises methods and results published in the original papers Zheng et al. "Extracellular Vesicles Derived from Neural Progenitor Cells--a Preclinical Evaluation for Stroke Treatment in Mice" and Haupt M, Zheng X, et al."Lithium modulates miR-1906 levels of mesenchymal stem cell-derived extracellular vesicles contributing to poststroke neuroprotection by toll-like receptor 4 regulation"

Contents

Abbreviations	IV
1 Introduction	1
1.1 Epidemiological and clinical aspects of ischemic stroke.....	1
1.2 Endogenous neurogenesis and stem cell transplantation	2
1.3 Extracellular vesicles (EVs) and stroke.....	4
2 Aim of the study.....	6
3 Materials and Methods	7
3.1 Legal issues, animal housing, randomization and blinding.....	7
3.2 Primary culture of NPCs and MSCs	7
3.3 Isolation of EVs from NPCs and MSCs	8
3.4 EV characterization.....	11
3.5 Analysis of EV cargo	11
3.6 Cerebral organoids and oxygen-glucose-deprivation (OGD) assay	12
3.7 Experimental paradigm and animal groups.....	12
3.8 Statistical analysis.....	15
4 Results and discussion.....	16
4.1 Characterization of NPC-EVs.....	16
4.2 NPC-EVs are neuroprotective in cerebral organoids exposed to OGD	19
4.3 NPC-EV administration stimulates poststroke neuroregeneration and axonal plasticity in vivo	23
4.4 NPC-EVs predominantly distribute in peripheral organs and reverse peripheral poststroke immunosuppression.....	29
5 References	35
6 Copy of the Publication 1.....	42

Abbreviations

BDA	biotinylated dextran amine
BDNF	brain-derived neurotrophic factor
BrdU	bromodeoxyuridine / 5-bromo-2'-deoxyuridine
DCX	doublecortin
EGF	epidermal growth factor
EV	extracellular vesicle
FGF	fibroblast growth factor
HGF	hepatocyte growth factor
HSP70	70 kilodalton heat shock protein
IDO	indoleamine 2,3-dioxygenase
MCA	middle cerebral artery
MCAO	middle cerebral artery occlusion
MSC	mesenchymal stem cell
NPC	neural progenitor cell
NSC	neural stem cell
NTA	nanoparticle tracking analysis
OGD	oxygen-glucose deprivation
PEG	polyethylene glycol
RT	room temperature
SVZ	subventricular zone
TEM	transmission electron microscopy
TUNEL	terminal deoxynucleotidyl transferase dUTP nick end labeling
VEGF	vascular endothelial growth factor
PDGF-D	platelet-derived growth factor D

1 Introduction

1.1 Epidemiological and clinical aspects of ischemic stroke

According to data obtained from the World Health Organization, stroke was the second leading cause of death worldwide in 2019. The disease causes of stroke can be differentiated into either hemorrhagic or ischemic forms of stroke. With about 85% of all strokes being ischemic, this kind of stroke is clinically more relevant than hemorrhagic strokes (Musuka et al. 2015). Hence, the present thesis focuses on ischemic strokes, also known as cerebral ischemia, and uses the term "stroke" in this context only.

Stroke is a disease of the elderly for which several risk factors such as carotid stenosis, hypertension, hyperlipidemia, and smoking exist (Boehme et al. 2017). Ischemic strokes can further be distinguished by their pathophysiology, among which are the formation of a thrombus or an embolus as well as systemic hypoperfusion. However, embolic and thrombotic strokes are the most common types of ischemic stroke.

Stroke therapy has made significant progress in the last decades because of the establishment of both systemic thrombolysis within 4.5 hours and endovascular treatment. Whereas thrombolysis has already been introduced in the 1990ies (Harder und Klinkhardt 2000), it was not before 2015 where endovascular treatment became a scientifically supported treatment paradigm (Starke et al. 2016). Nevertheless, most patients do not qualify for either treatment paradigm because of a restricted time window or significant side effects (Seitz 2016). Therefore, many patients suffer from low life quality after stroke, and different treatment paradigms are urgently needed. Although neuroprotective approaches have been successfully applied in the preclinical stroke models, their translation into the clinic has failed until recently (Gladstone et al. 2002).

Novel research strategies, therefore, focus on the development of neuroregenerative rather than neuroprotective paradigms.

1.2 Endogenous neurogenesis and stem cell transplantation

Whereas neuroprotection is only feasible at the acute stage of the disease, neuroregenerative approaches may be beneficial at subacute or even chronic stroke stages. Nevertheless, neuroregeneration upon stroke is not clearly defined and implies heterogeneous phenomena such as neurogenesis, angiogenesis, neural plasticity, and stem cell transplantation approaches. Endogenous neurogenesis is not restricted to the ontogenesis of the brain but also persists in defined stem cell niches of the adult brain, such as the subgranular zone of the dentate gyrus and the subventricular zone (SVZ) of the lateral ventricles (Kaneko et al. 2011). Under physiological conditions, endogenous astrocyte-like neural stem cells (NSCs) migrate along the rostral migratory stream towards the olfactory bulb, where they finally differentiate into mature neurons (Doetsch et al. 1999). Endogenous neurogenesis is also present in the human brain, an essential prerequisite for stroke therapy in men (Jin K et al. 2006).

Induction of cerebral ischemia stimulates endogenous neurogenesis, as is the case with other pathological conditions like neurodegenerative diseases or traumatic brain injury. Interestingly, endogenous neurogenesis can also be found in the brain of ischemic stroke patients (Jin K et al. 2006; Marti-Fabregas et al. 2010). In preclinical stroke models, NSCs migrate from the SVZ to the stroke area where they differentiate into mature neurons or glial cells (Yamashita et al. 2006), as indicated by increased expression patterns of doublecortin (DCX) or NeuN (Motamed et al. 2019). However, the therapeutic impact of poststroke endogenous neurogenesis is limited because of the low survival rates of these newborn cells; the majority of them die within weeks (Dayer et al. 2003; Kempermann et al. 2003). Additional strategies are needed in order to further enhance neuroregenerative mechanisms upon stroke induction. Such strategies imply a direct stimulation of neurogenesis and the transplantation of exogenous stem cells. Stimulating

endogenous neurogenesis aims at boosting cell growth, proliferation, mobilization, and cell differentiation (Bernstock et al. 2017).

Although the strategy mentioned before might appear to be attractive under certain conditions, the transplantation of exogenous stem cells appears to be more feasible. As a matter of fact, cell transplantation therapy has been expected to benefit patients suffering from a wide range of different diseases and injuries (Reisman und Adams 2014). Under stroke conditions, injecting exogenous stem cells into the lesioned striatum results in a better neurological outcome and increased neurogenesis levels (Zhang GL et al. 2019), observations which have also been made with other stem cell sources such as embryonic stem cells, MSCs, and induced pluripotent stem cells (Liu et al. 2020).

Although the precise mechanisms by which stem cells such as MSCs induce tissue regeneration are not entirely understood, there are various mechanisms involved. As such, mitochondrial or exosomal transfer from transplanted MSCs towards the extracellular environment has recently been described (Li et al. 2019). Consequently, MSCs can directly or indirectly modulate the extracellular environment by interfering with growth factors or inflammatory signaling cascades. Both TNF- α and NF- κ B expression levels are regulated in hypoxic neuronal cells and animal stroke models due to MSCs, which results in a stimulation of vascular endothelial growth factor (VEGF) related pathways and reduced apoptotic cell death (Huang et al. 2014). Reduction of NF- κ B expression due to MSCs also reduces inflammatory response after stroke (Gu et al. 2014). Likewise, human umbilical cord blood MSCs decrease brain injury in a preclinical stroke model by reducing IL-17 and IL-23 expression (Ma et al. 2013). Regulation of inflammation by MSCs in stroke settings affects the peripheral and central nervous system. Hence, MSCs inhibit microglial activation and decline astrogliosis formation within the ischemic stroke brain, a way of action that implies non-classical JAK-STAT signaling with non-phosphorylated signal transducer and activator of transcription 3 in immune cells (Wang HZ et al. 2019).

MSCs administration can stimulate astrocytes to release growth factors such as VEGF, epidermal growth factor (EGF), and bFGF in cerebral ischemia (Zhu et al. 2015). The grafted MSCs can normalize aquaporin-4 expression and suppress the apoptosis process in ischemic astrocytes. Interestingly, MSCs also help preserve the integrity of the blood-brain barrier (BBB) by stimulating astrocytes to produce growth factors such as VEGF, EGF, and bFGF within the stroke brain (Tang G et al. 2014).

The aforementioned MSC-induced effects depend on various parameters and appear to be indirect. As a matter of fact, administration routes significantly impact stem cell transplantation efficiency (Doepfner et al. 2015a), with directly injected stem cells into the stroke lesion rather not affecting the immune system at all (Chrostek et al. 2019). However, clinically more favorable systemic stem cell transplantation does not directly affect neurogenesis in the lesioned tissue but prevents poststroke immunosuppression, a leading cause of infection in stroke patients (Chrostek et al. 2019). Despite these favorable therapeutic effects of stem cells in general, research questions the necessity of stem cell transplantation for stroke (Borlongan 2019; Singh et al. 2020). Instead, most biological functions observed due to stem cell transplantation appear to be the result of extracellular vesicles (EVs) that are secreted from these stem cells, making cell transplantation an unnecessary risk for the recipient.

1.3 Extracellular vesicles (EVs) and stroke

As stated before, MSCs and other stem cells appear to exert their biological impact by secreting EVs under both physiological and pathological conditions alike. EVs are a miscellaneous group of lipid bilayer structures that are secreted from virtually all cells (Carpintero-Fernandez et al. 2017). The diameter of EVs is between 30 nm and 1000 nm. In terms of size, EVs can be divided into small EVs (less than 200 nm) and large EVs (They et al. 2018). Because most of the reports published do not distinguish small EVs or large EVs, the term EVs to refer to small

EVs or large EVs is used. EVs achieve their biological functions by various cargos, i.e., RNAs, DNAs, and proteins (Doyle und Wang 2019).

As is the case for MSCs, most EV data in the stroke research field comes from MSC-EVs. Several studies have suggested that EVs may indeed be biologically relevant mediators of stem cells, and preclinical data from the use of stem cell-derived conditioned media depict similar effects in *in vitro* and *in vivo* stroke models (Doeppner et al. 2017a; Egashira et al. 2012; Yang et al. 2018). Whereas initial hypotheses focused on soluble factors inside the conditioned medium being the biologically active mediator, the recent scientific focus has now switched towards the aforementioned EVs. Indeed, a substantial amount of preclinical reports have convincingly shown that EVs are beneficial in stroke and other disease models (Harrell et al. 2019; Hill 2019; Keshtkar et al. 2018; Kubo 2018). MSC-EVs have been shown to promote functional recovery and neurovascular plasticity (Xin et al. 2013) and neurogenesis in the ischemic stroke model (Ophelders et al. 2016; Zhang Y et al. 2017). Likewise, previous research from our group showed that MSC-EVs promote poststroke neurogenesis in a rodent stroke model, possibly via a mechanism involving the restoration of postischemic peripheral immunosuppression (Doeppner et al. 2015b). Whereas plenty of different stem cells can be used to improve neurological recovery in preclinical and even some clinical settings (Chrostek et al. 2019; Joers und Emborg 2009), it is uncertain whether or not the beneficial effects described before on MSC-EVs will hold for EV species from other cell sources, including neural progenitor cells (NPCs). Hence, it is elusive if EVs are feasible for being a general therapeutic concept or only being beneficial when derived from distinct cell types such as MSCs.

2 Aim of the study

EVs have subsequently been shown to protrude various beneficial therapeutic effects in many disease models, including cerebral and myocardial ischemia, lung injury, and kidney injury (Gatti et al. 2011; Lai et al. 2010; Xin et al. 2013). These results have exclusively been obtained through MSC-EVs. On the contrary, stem cell stroke studies were not only limited to MSC transplantation, but also included other stem cell sources like NPCs (Bacigaluppi et al. 2009; Doeppner et al. 2010; Rumajogee et al. 2018; Wilcox et al. 2014; Zhang P et al. 2011). In contrast, the therapeutic potential of NPC-EVs under stroke conditions has not been explored to date. Even though EVs seem to be a fascinating tool for adjuvant stroke therapy, fundamental questions still need to be addressed, including the relevance of host cells for EV harvesting. Therefore, the present thesis aimed to evaluate the therapeutic potential of NPC-EVs in an *in vitro* and *in vivo* stroke model in comparison to well established MSC-EVs.

3 Materials and Methods

3.1 Legal issues, animal housing, randomization and blinding

In compliance with EU rules, all animal experiments were subject to local authority approval. The ARRIVE standards were adhered to for the treatment and use of laboratory animals. The mice were kept under a circadian rhythm in groups of five each and had free access to food and water. All animals were randomly assigned to the various experimental groups. For all phases of the study, the experimenter was blinded to the treatment protocols.

3.2 Primary culture of NPCs and MSCs

P1 mice for the preparation and isolation of NPCs were euthanized using an overdose of CO₂ followed by decapitation (Guo et al. 2012). Skin and skull were removed with forceps. The brain was carefully separated, and the meninges were carefully removed from the brain, while the cerebellum was discarded. The SVZ from the brains of P1 mice was isolated in cold PBS on ice. After that, the tissue was centrifuged to precipitate the tissue. The supernatant was removed, and the SVZ tissue was cut into small pieces and digested with trypsin-EDTA. The tissue tubes were gently shaken in a 37°C water bath for 15 minutes. NPC medium (the contents of the neural progenitor cell medium can be found in **Publication 1**) was added to terminate the digestion. The precipitate and NPC medium were mixed by gentle vortex and then centrifuged at room temperature (RT) for 15 minutes. The supernatant was discarded, and the precipitate was washed three times with NPC medium, and each wash was centrifuged at 200x g at RT for 5 minutes. The NPC precipitation sample was finally resuspended in 2 ml of complete NPC medium and then inoculated into Petri dishes containing 3 ml of complete NPC medium. The formation of neurospheres was continuously controlled over a 72-hour period. Every three days, additional growth factors were added to the Petri dishes. Cells were passaged every 5 to 6 days (details can be found in **Publication 1**).

MSCs were obtained from the fatty tissue of adult C57BL/J male mice. Mice were sacrificed under anesthesia with an overdose of isoflurane and by cervical dislocation. The adipose tissue was carefully separated from the retroperitoneum, groin, epididymis, and brown adipose tissue on the armpit with forceps and scissors. The tissue was centrifuged in 15 ml PBS at 100x g for 2 minutes at RT for precipitation purposes. The supernatant was discarded after centrifugation, and the precipitation was digested with 20 ml of PBS containing 10 g of type 1 collagenase (Sigma-Aldrich, St. Louis, MO, USA) and incubated in a 37°C water bath for 15 minutes. After type 1 collagenase digestion, the centrifuge tubes containing digested tissue were centrifuged at 500x g for 8 minutes at RT. The supernatant was discarded, and precipitation was resuspended in pre-warmed PBS containing 1% BSA followed by centrifuged at 300x g for 5 minutes. The supernatant was discarded and resuspended the pellet with 10 ml of MSC medium. Primary MSCs were inoculated in T75 flasks containing 20 ml of complete MSC medium (with FBS). Each flask containing 3.6×10^6 MSCs was incubated at standard cell culture conditions at 37°C in a humidity of 95% containing 5% CO₂. The MSCs were passaged every 6 to 7 days. The details of MSC isolation can be found in **Publication 1**.

3.3 Isolation of EVs from NPCs and MSCs

There are many EV isolation methods. However, the optimal isolation method for EVs is still under debate (Buschmann et al. 2018). Due to the ability of the polyethylene glycol (PEG) method to process a large number of cultures simultaneously, the method can effectively address the need for large numbers of EVs for future clinical applications. Therefore, I have chosen this method as our EV extraction method. However, the PEG method is also considered a "high contamination" method because PEG can co-precipitate organelles and soluble proteins. We, therefore, have chosen the ultracentrifugation only method as our purity control. The difference between the ultracentrifugation only method and the PEG method is that the ultracentrifugation only method did not contain PEG in the collected culture medium. The cells, cell debris, and apoptotic bodies were removed by filtration and then directly ultracentrifuged. The details about

the isolation method can be found in **Publication 1**. The different isolation methods have upside and downside aspects, and a summary of each of them can be found in table 1.

Table 1. Advantages and disadvantages of different extracellular vesicle (EV) isolation techniques.

Technique	Advantage	Disadvantage	Reference
Ultracentrifugation only	low costs, high purification rates	time-consuming, potential EV damage	— They et al. 2006
nanomembrane or filters	handling of large volumes, low centrifugation speed	high cost, contamination by proteins, deformation of EVs	— Lobb et al. 2015
size-exclusion chromatography	reproducibility and purity, high sensitivity, no additional chemicals	high costs, limited sample volume	— Lobb et al. 2015
precipitation with polymers	low costs, simple protocol, can handle large volumes	protein and other contamination	— Ludwig et al. 2018
microfluidic technologies	rapidness, purity, efficiency	high costs need special equipment	— Nakai et al. 2016

3.4 EV characterization

According to the International Society for Extracellular Vesicles guidelines, the characterization of EVs needs to include three different aspects, i.e., protein markers, size, and morphology (Thery et al. 2018). Herein, the proteins CD63, Alix, and TSG101 were chosen as EV positive markers for Western blotting, whereas calnexin served as a negative marker. Of note, some restrictions apply to calnexin in this context, as will be addressed later in this document. For size determination and quantitative analysis of enriched NPC-EVs, a nanoparticle tracking analysis (NTA) was performed by using the Nanosight platform (Particle Metrix, Inning am Ammersee, Germany). As EVs are all on the nanoscale, ordinary fluorescence microscopy cannot confirm their microscopic structure. As such, transmission electron microscopy (TEM) was performed for the identification of the microstructure of EVs. The TEM experiments were exclusively performed by Dr. Möbius from the Max Planck Institute for Experimental Medicine, Göttingen. The details of the NTA measurement, TEM, and Western Blot protocols can be found in **Publication 1**.

3.5 Analysis of EV cargo

As described before, EVs achieve their biological functions by transferring their contents such as RNA and proteins towards the extracellular environment or directly to neighboring cells. Hence, the protein contents of NPC-EVs were analyzed using mass spectrometry. In brief, the EV samples were separated on 4-12% gels and cut into 12 equidistant lanes. The gel pieces were digested with trypsin overnight and were dried the next day for mass spectrometry analysis. Besides the protein contents, miRNAs are also key players of EVs for achieving biological functions. Several miRNA candidates that showed neuroprotective effects in ischemic stroke models were investigated by qRT-PCR. The mass spectrometry analysis was performed by Dr. Christof Lenz from the UMG's Core Facility Proteomics. The details of mass spectrometry analysis and qRT-PCR can be found in **Publication 1**. PCR primers and U6 were bought from

Eurofins Genomics (Luxembourg, Luxembourg). U6 was used as an internal control; the primer sequence and miRNA candidates can be found in **Publication 1**.

3.6 Cerebral organoids and oxygen-glucose-deprivation (OGD) assay

Like drugs, the dosage of EVs may affect the therapeutic effect. However, the optimal EV concentration has not yet been determined, which was therefore done for NPC-EVs herein. Since traditional cell cultures only insufficiently reflect the complicated *in vivo* situation, so-called cerebral organoids were used as an *in vitro* model of the brain. The cerebral organoids were kindly provided by Dr. Zafeiriou from the Institute of Pharmacology and Toxicology of the UMG. The details on cerebral organoids are mentioned in **Publication 1**. First, the optimal OGD settings, i.e., the duration of OGD, were determined for these cerebral organoids. Thereafter, different NPC-EV concentrations defined as low, medium, and high were chosen to study the optimal NPC-EV concentration for the specific OGD condition. Terminal deoxynucleotidyl transferase dUTP nick end labeling (TUNEL, *in situ* cell death detection kit, Merck Group) staining was used to detect cell death according to its instructions, with 4', 6-diamidino-2-phenylindole (DAPI) staining used for the detection of cell nuclei. The details of the OGD model protocol can be found in **Publication 1**.

3.7 Experimental paradigm and animal groups

Having obtained data on the optimal concentration of EVs in the *in vitro* experiments, the transfer towards the middle cerebral artery occlusion (MCAO) mice model was done (Doepfner et al. 2015b). Briefly, mice were anesthetized with 3% isoflurane, and the internal carotid artery (ICA), external carotid artery (ECA), and common carotid artery (CCA) were carefully separated, permanently ligating the proximal ends of the ECA and the CCA. Next, the left ICA was temporarily clamped with an arterial clip, and a small incision on the left CCA was cut. The silicon-coated monofilament (Doccol Corp., Sharon, MA, USA) was carefully inserted into the left CCA and then softly pushed into the ICA until it reached the left middle cerebral artery

(MCA). Reperfusion was started by removing the monofilament 60 minutes after insertion. In this *in vivo* experiment, three different EV concentrations were used for NPC-EVs and MSC-EVs. A total of seven groups was generated, i.e., Saline (control), NPC-EVs low (EVs equivalent 2×10^5 NPCs), MSC-EVs low (EVs equivalent 2×10^5 MSCs), NPC-EV medium (EVs equivalent 2×10^6 NPCs), MSC-EV medium (EVs equivalent 2×10^6 MSCs), NPC-EV high (EVs equivalent 2×10^7 NPCs), and MSC-EV high (EVs equivalent 2×10^7 MSCs).

The therapeutic impact of such applied EVs was analyzed both on the histological level and the behavioral level. The latter included the corner turn test, the balance beam test, and the tight rope test to evaluate poststroke motor coordination. Mice were trained on days 1 and 2 before inducing MCAO to confirm proper test behavior before stroke induction. For the tight rope test, a score sheet was used to evaluate the tight rope test results (details in **Publication 1**) as first mentioned previously (Doeppner et al. 2011). On the histological level, neuroregeneration was measured as indicated by increased levels of neurogenesis in the ischemic brain. For this purpose, animals were treated with the proliferation marker BrdU, and cells were post mortem counterstained against DCX (immature neuronal marker) or NeuN (mature neuronal marker). Axonal plasticity was assessed using the anterograde tract tracer biotinylated dextran amine (BDA), which was applied 70 days poststroke into the contralateral undamaged cortex stereotaxic injection.

According to our previous studies, EVs modify the poststroke immune system and thus have an immunomodulatory effect. Flow cytometry was applied to investigate the effect of NPC-EVs on the central and the peripheral immune system (the details about flow cytometry can be found in **Publication 1**). FlowJo v10.0 software was used to analyze the data from flow cytometry experiments. The latter was a courtesy from the workgroup of Prof. Dr. med. Martin S. Weber, Neurology/Neuropathology, UMG.

Distribution patterns of NPC-EVs within the rodent organism were studied using a cell tracker dye to label EVs before injection into the animals. Injections were performed via a femoral vein

injection or retro-orbital injection of sham animals or MCAO animals. The details of the *in vivo* experiments can be found in **Publication 1**. The experimental paradigm is also summarized in **Figure 1**.

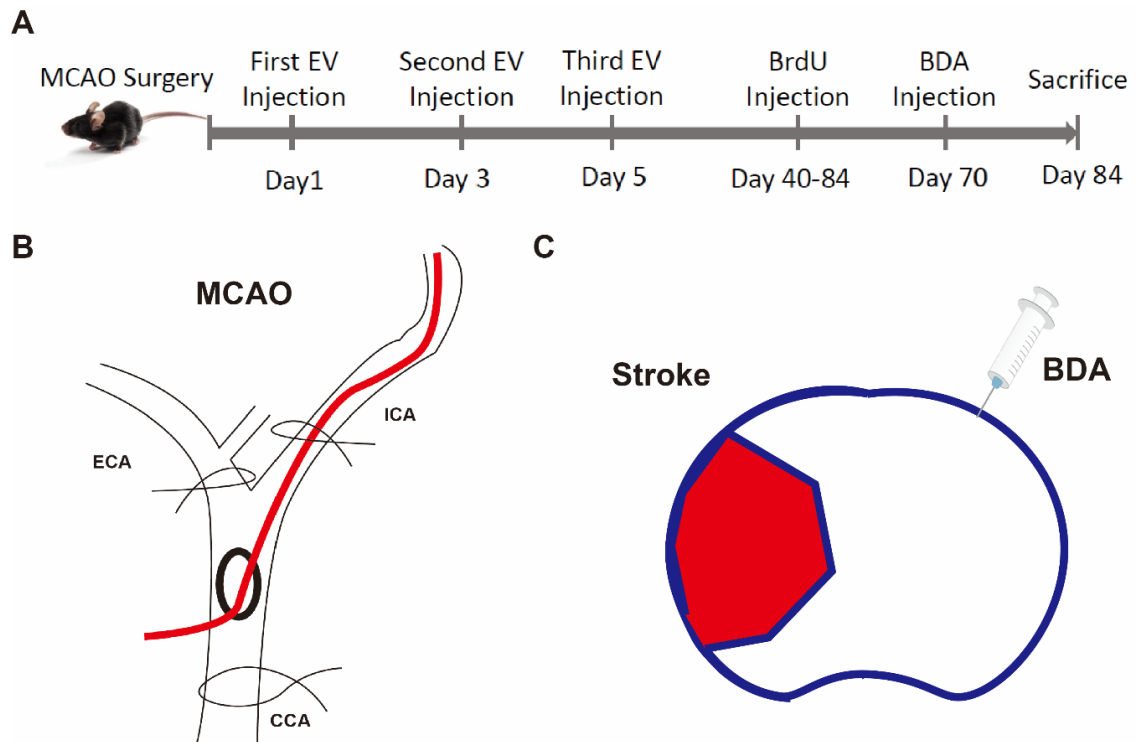


Figure 1. Experimental paradigm, middle cerebral artery occlusion, and BDA injection. **A.** The mice received an EV injection 1 day, 3 days, and 5 days after MCAO. The behavior tests were performed on days 7, 14, 28, 56, and 84 after MCAO. **B.** Schematic diagram of the MCAO surgery. The ICA, ECA, and CCA were carefully separated, permanently ligating the proximal ends of the ECA and the CCA. The left ICA was temporarily occluded, and the monofilament was carefully inserted into the left CCA through a small incision on the CCA. The monofilament was gently pushed into the ICA until it reached the left MCA. **C.** The anterograde tract tracer biotinylated dextran amine (BDA) was injected into the contralateral non-ischemic cortex by stereotactic injection on day 70 poststroke to investigate axonal plasticity. Abbreviations: EV = extracellular vesicle, BDA = biotinylated dextran amine, ICA = internal carotid artery, ECA = external carotid artery, CCA = common carotid artery, MCAO = middle cerebral artery occlusion. The elements in this figure are creative commons (CC BY 3.0).

3.8 Statistical analysis

In order to compare two groups, the two-tailed independent Student's t-test was used. For analysis of three or more groups, a one-way study of variation (ANOVA) was accompanied by a Tukey's post-hoc-test. Unless otherwise mentioned, data are viewed as mean with SD values. A *p*-value of less than 0.05 was considered to be significantly different. Statistical analysis was done using Graphpad Prism version 8.

4 Results and discussion

4.1 Characterization of NPC-EVs

The recent finding on stem cells acting indirectly through EV secretion has revolutionized many scientific fields, among which is the experimental stroke field (Harrell et al. 2019; Hill 2019; Keshtkar et al. 2018; Kubo 2018). Nevertheless, data on EVs in preclinical stroke settings most exists for MSCs (Ophelders et al. 2016; Zhang Y et al. 2017). Whether or not EVs are a general concept for future adjuvant stroke therapy and related diseases is of uttermost importance. Hence, the therapeutic value of NPC-EVs was analyzed using both an *in vitro* and *in vivo* stroke model. Following the International Society for Extracellular Vesicles guidelines, however, NPC-EVs were first *in vitro* characterized before being used in the stroke models (They et al. 2018).

Although PEG is often used for the enrichment of EVs, it is considered to yield highly contaminated samples since it forms a web-like structure in which it is trapped. During this process, some soluble macromolecules of protein may also be precipitated in this process. In addition, PEG precipitation may also form agglomerates at the microscopic level, increasing the size of EVs and decreasing the efficacy of EVs. Measuring EV positive markers such as Alix, TAPA1, TSG101, and CD63 in both PEG samples and ultracentrifugation only samples (ultracentrifugation only method is still regarded as the gold standard for EV enrichment), the expression level of EV positive markers did not differ between the two isolation methods (**Figure 2. A, B**). Analyzing the size distribution using NTA and the morphology using TEM also did not give rise to any statistical difference (**Figure 2. C, D**). Of note, TEM analysis did not reveal any EV agglomeration in the PEG approach.

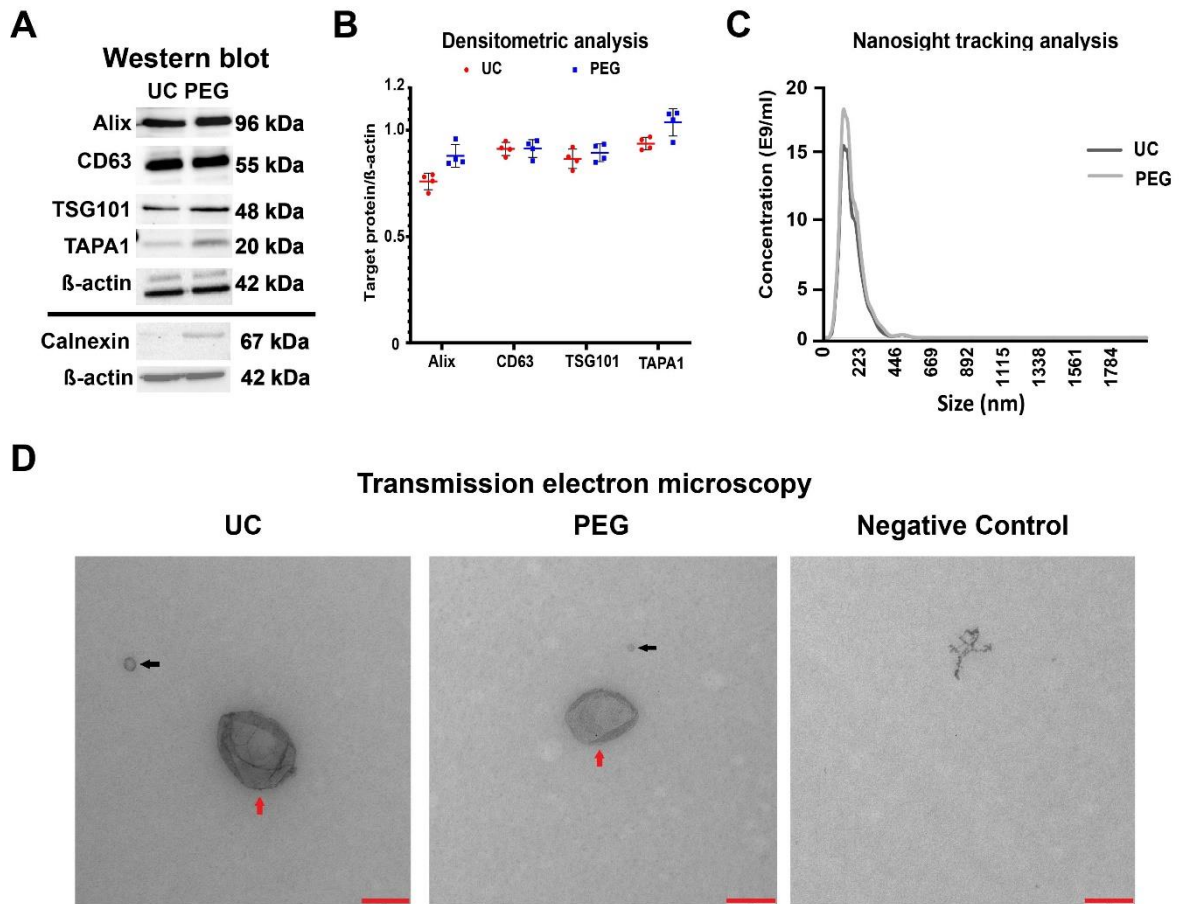


Figure 2. Characterization of NPC-derived EVs. **A.** Characterization of EV biological markers by Western blot. Alix, Cd63, and TSG101, which are related to the biogenesis of EVs, were identified in NPC-EVs. **B.** Quantification of Western blot from **A.** No differences between PEG and UC methods in EV biological marker expression were detected. **C.** Nanosight tracking analysis showing the size distribution of NPC-EVs of different isolation methods. There was no significant difference between the two isolation methods in EV size distribution. **D.** Transmission electron microscopy image of NPC-EVs of different isolation methods. Negative control is PBS only. Red arrow pointed to the microvesicle and black arrow pointed to the exosome. Scale bar: 200 nm. Abbreviations: EV, extracellular vesicles; PBS, phosphate-buffered saline; PEG, polyethylene glycol; NPC, neural progenitor cell; NTA, insight tracking analysis; TEM, transmission electron microscopy; UC, ultracentrifugation.

Further characterization of NPC-EVs included an analysis of expression patterns of EV specific markers, more EV positive markers were detected and no statistically significant difference was found between the two isolation methods (**Figure 3. A, B, C**). Furthermore, negative markers such as UMOD, APOA1, and ALB were not detected after mass spectrometry analysis (**Figure**

3. **D**). Since PEG isolation may also result in co-precipitation of extracellular miRNAs, expression levels of miRNA candidates were analyzed. Again, no statistically significant difference was observed between the two isolation methods (**Figure 3. E**).

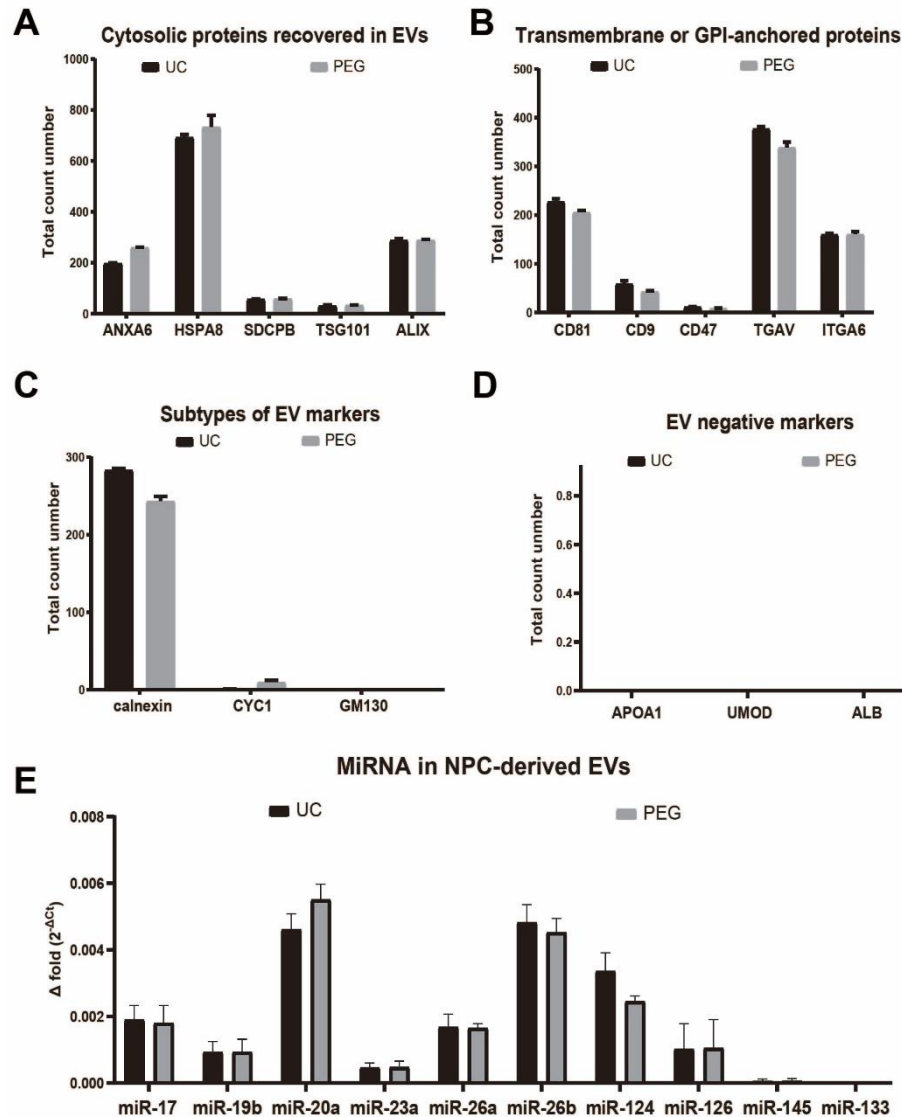


Figure 3. Mass spectrometric analysis and qRT-PCR analysis of selected proteins and miRNAs in NPC-derived EVs. A, B, C Proteomic analysis of NPC-EVs. Typical EV markers such as ANXA6, CD81, GM130 etc. were found in NPC-EVs, and no difference between the two isolation methods was detected. **D.** EV negative control biomarkers were not detected in both isolation methods. **E.** miRNA expression in NPC-EVs. Several miRNAs related to neuroprotection or neurogenesis were found in NPC-EVs. The miRNAs in NPC-EVs were detected by qRT-PCR. The quantification of qRT-PCR was using the $2^{-\Delta Ct}$ method. Abbreviations: EV, extracellular vesicles; PBS, phosphate-buffered saline; PEG, polyethylene

glycol; NPC, neural progenitor cell; NTA, insight tracking analysis; TEM, transmission electron microscopy; UC, ultracentrifugation.

These data provide evidence that the PEG method used in the present experimental paradigm is not inferior to the differential ultracentrifugation technique about sample purity. This first conclusion is critical for the remainder of the study, since PEG allows processing of large sample volumes efficiently compared to the ultracentrifugation only method. Additional experiments were therefore performed using PEG isolated EVs only.

4.2 NPC-EVs are neuroprotective in cerebral organoids exposed to OGD

In order to establish the OGD model of cerebral organoids, the optimal duration of hypoxia followed by reoxygenation of 24 hours was determined. Compared to cerebral organoids kept at standard cell culture conditions without hypoxia, OGD duration for 8 hours or 10 hours yielded a cell death rate of 80% or 83%, respectively. Since these cell death rates were similar, further experiments were done using the 8-hour OGD time window only.

Thereafter, the optimal NPC-EV concentration was defined for the aforementioned experimental setting. Using the TUNEL assay, NPC-EV administration resulted in a profound and robust neuroprotective effect for all three EV concentrations when compared to the solvent control (**Figure 4. A, B, C**).

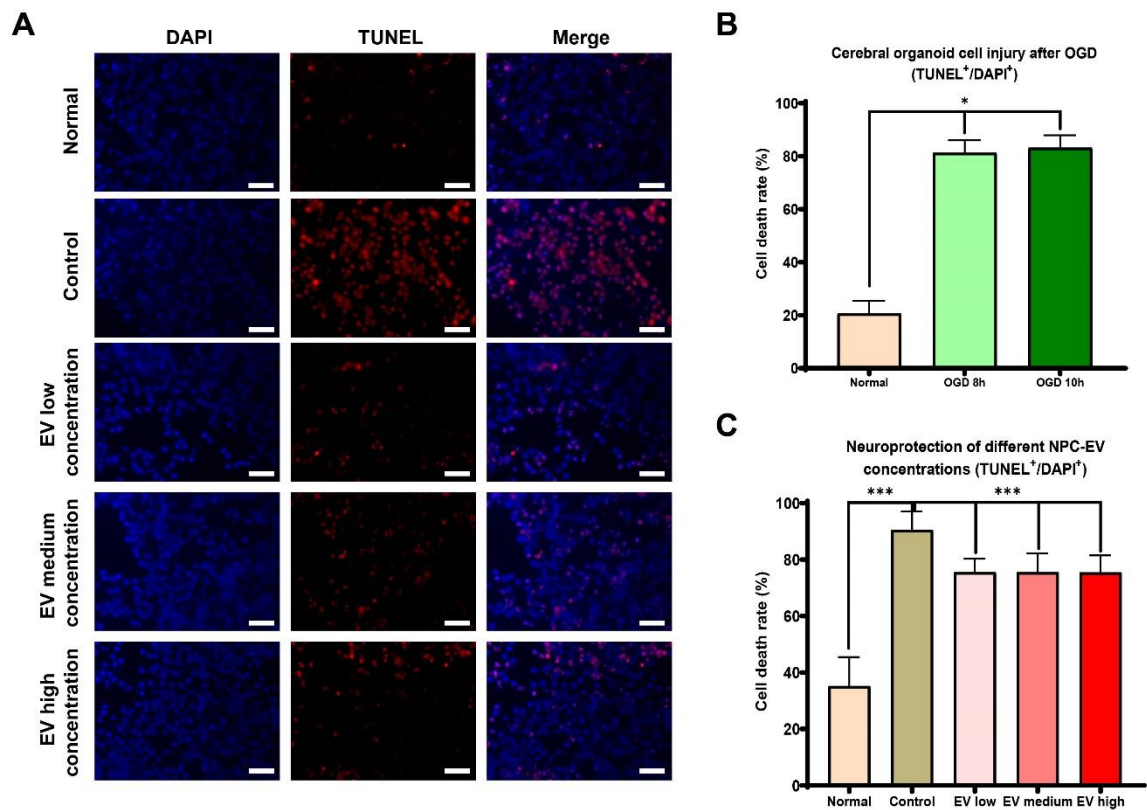


Figure 4. NPC-EVs are neuroprotective in cerebral organoids exposed to OGD. A. Representative photos from EV-treated cerebral organoids. **B.** The temporal resolution of the development of cell death under OGD conditions was determined for cerebral organoids ($n=3$ per condition) exposed to 8 h or 10 h of OGD, followed by reoxygenation under standard cell culture conditions for an additional 24 h. Cell death rates were assessed using TUNEL staining on cryosections, with DAPI staining for nuclear detection. Since no statistical significance of cell death rates of organoids exposed to either 8 h or 10 h of OGD was observed, further experiments were done only using the 8 h time window. **C.** Organoids were treated with NPC-derived EVs at the beginning of the OGD and additionally at the beginning of the reoxygenation. Three different NPC-EVs dosages were chosen ($n=3$ per condition), i.e., NPC-EVs low (EVs equivalent to 2×10^5 NPCs), NPC-EVs medium (EVs equivalent to 2×10^6 NPCs), and NPC-EVs high (EVs equivalent to 2×10^7 NPCs). Control organoids were exposed to OGD only without EV treatment, whereas "normal" refers to cerebral organoids kept under standard cell culture conditions. Scale bars: 20 μm . *: $p < 0.05$, **: $p < 0.005$, ***: $p < 0.0005$, compared to control. Abbreviations: EV, extracellular vesicles; OGD, oxygen-glucose-deprivation; PBS, phosphate-buffered saline; NPC, neural progenitor cell; TUNEL, terminal deoxynucleotidyl transferase dUTP nick end labeling.

The fact that EVs induce immediate neuroprotection in an *in vitro* stroke model is not trivial. *In vitro* models lack the immune system that *in vivo* models have. As a matter of fact, *in vivo* stroke data is in favor of EVs regulating poststroke immune responses rather than reducing brain injury or infarct volumes directly (Doepfner et al. 2015b). As such, the next experiments focused on analyzing possible cargo proteins or miRNAs that might yield these beneficial effects. Using both literature databases as well as previous work from our own group, multiple miRNAs and proteins were identified in NPC-EVs that are associated with neuroprotection. Among these notable candidates are miR-124, microRNA 17-92 cluster, 70 kilodalton heat shock protein (HSP70), and VEGF (Supplementary data in **Publication 1**). The miRNA 17-92 cluster and the miR-124 that are found in NPC-EVs are well known for their neuroprotective and neurogenesis effects as shown in many studies that are independent from EV application (Doepfner et al. 2013b; Hamzei Taj et al. 2016; Jin J et al. 2018; Matsuoka et al. 2018; Pan et al. 2019; Saraiva et al. 2018; Yang J et al. 2017; Yang P et al. 2017). These cargo miRNAs might thus have a direct impact in the OGD cerebral organoid model which has been so far been unbeknownst. Although the precise mechanisms that may underly these effects are not known, it is likely that EVs transfer such cargo to the target cells in question (Abels und Breakefield 2016).

EVs do not contain miRNAs only, and both the mass spectrometric analysis and the Western blotting revealed high expression patterns of distinct protein candidates such as HSP70 and VEGF, which may also contribute to NPC-EV-induced neuroprotection. These two proteins are well known to be involved in a plethora of signaling cascades, among which are pathways that help increase neuronal resistance under hostile hypoxia/ischemia conditions (Giffard und Yenari 2004; Jiang et al. 2020; Wang Y et al. 2005). Under *in vivo* conditions, for instance, HSP70 increases cell viability and improves nervous system recovery by modifying oxidative stress and proteasome activity in brain tissue exposed to ischemic injury. (Doepfner et al. 2013a; Doepfner et al. 2009; Doepfner et al. 2017b; Doepfner et al. 2012). Thus, the increased resistance of brain-like organs exposed to OGD injury treated with NPC-EVs might also be in

part due to an HSP70-dependent regulation of proteasomal activity. Measurement of proteasome activity, however, was beyond the scope of the present work.

Further proteomic analysis of NPC-EVs gave rise to several pathways in which NPC-EVs may be involved, such as the mTOR signaling pathway and the PTEN related pathway. A summary of such NPC-EV-related signaling pathways that may be affected in the process of NPC-EV-induced neuroprotection is given in table 2. Among these pathways, the EGF pathway and the PDGF pathway are the ones that have been shown to have a direct relationship with neuroprotection and regeneration. The EGF pathway is deeply involved in cell proliferation and survival. EGF can promote neural regeneration by improving the cerebral microenvironment after stroke (Chan et al. 2019). The platelet-derived growth factor (PDGF) related pathway protects neurons through a variety of mechanisms. In addition to directly inhibiting NMDA receptors, PDGF can also protect neurons from an ischemic condition by upregulating the expression of downstream pro-survival genes such as GSK3 β and PI3K/AKT (Tang Z et al. 2010).

Pathway	Related Gene count
Rho cell motility signaling pathway	17
Integrin Signaling Pathway	17
Signaling of Hepatocyte Growth Factor Receptor	17
How Progesterone Initiates the Oocyte Maturation	16
Skeletal muscle hypertrophy is regulated via AKT/mTOR pathway	15
mTOR Signaling Pathway	15
Erk and PI-3 Kinase Are Necessary for Collagen Binding in Corneal Epithelia	15
Transcription factor CREB and its extracellular signals	14
EGF Signaling Pathway	14
Y branching of actin filaments	13
Multiple antiapoptotic pathways from IGF-1R signaling lead to BAD phosphorylation	13
Phospholipids as signalling intermediaries	13
PDGF Signaling Pathway	13
Regulation of eIF4e and p70 S6 Kinase	12
mCalpain and friends in Cell motility	12
Role of ERBB2 in Signal Transduction and Oncology	12
TPO Signaling Pathway	12
Trefoil Factors Initiate Mucosal Healing	12
PTEN dependent cell cycle arrest and apoptosis	11
Apoptotic Signaling in Response to DNA Damage	11
Inhibition of Cellular Proliferation by Gleevec	11
Regulation of BAD phosphorylation	11
Role of PI3K subunit p85 in regulation of Actin Organization and Cell Migration	10
ER-associated degradation (ERAD) Pathway	10
AKAP95 role in mitosis and chromosome dynamics	9

Table 2. Signaling pathways potentially being involved in NPC-EV-induced neuroprotection Possible intracellular pathways regulated by NPC-EV inferred from an analysis of NPC-EV proteomic data. The database used for analysis is BIOCARTA.

Figure 5. Delivery of NPC-EVs reduces post-ischemic motor coordination impairment.

A. Balance beam test mainly focuses on testing the mobility recovery after MCAO surgery with or without EV treatment. All the EV concentration groups showed significant improvement on days 7, 14, 28 after EV administration. However, no significant difference was found after 56 days. **B.** Tight rope test focuses on forelimb strength and coordination recovery. All the EV groups showed significant improvement after seven days of EV administration compared to the control group, and the effects lasted till 84 days. **C.** The corner turn test focuses on detecting sensorimotor and postural asymmetries. All the EV groups showed significant improvement in sensory recovery from day 7 to day 84 after EV administration. **D.** The laser doppler graph showed the blood drop during MCAO surgery in each group. Scale bars: 20 μm . *: $p < 0.05$. Abbreviations: BrdU, 5-Bromo-2-deoxyuridine; DAPI, 4',6-diamidino-2-phenylindole; Dcx, doublecortin; EV, extracellular vesicles; MSC, mesenchymal stem cells; NPC, neural progenitor cell; PBS, phosphate-buffered saline.

The medium-dose group was more effective than the low and high dose groups in terms of motor function recovery. The reason for this is likely due to the formation of emboli in the NPC-EV high-dose group, whereas the low dose group may reach insufficient blood and tissue concentrations. The latter will ultimately result in an insufficient supply of biologically active cargo such as miRNAs, HSP70 and others towards the target cell. In the tight rope test, all NPC-EV and MSC-EV groups significantly improved the outcome from day 7 to day 84 (**Figure 5 B**). However, in the corner turn test, a test that mainly focuses on sensorimotor and postural asymmetries, showed significant improvement from day 7 to day 84 in the medium-dose of both NPC-EVs and MSC-EVs (**Figure 5 C**). One of the reasons for that might be because of the different focus on these two behavior tests. The corner turn test primarily approaches on testing the deficits of sensorimotor and postural asymmetries, while the tight rope test mainly focuses on the forelimb function and placing deficits. The different sensitivity aspects of different behavior tests cause differences in different concentration groups (Schaar et al. 2010).

In the balance beam test, the medium-dose group only showed effects in the balance beam test from 7 to 28 days. After 28 days, all the groups, including the control group, showed no significant difference compared to the control group (**Figure 5 A**). Since the balance beam test

mainly focuses on motor balance and coordination, the medium dosage of EVs had beneficial effects at the beginning of the poststroke condition. However, it would not accelerate the recovery rate of motor balance and coordination in the long-run. Interestingly, combining the behavior test results, only the medium dosage of NPC-EVs and MSC-EVs can improve the sensorimotor, postural asymmetries, forelimb function in the long-run but only yields a transient effect in motor balance and coordination recovery. Of note, MSC-EVs and NPC-EVs were derived from different cell sources. However, the same dosage achieved identical effects, suggesting that the dosage of stem cell-derived EVs but not the source of stem cell-derived EVs is the critical factor in improving the functional recovery. Unfortunately, research data on EV dose-dependent effects are limited. Tabak and his colleagues showed that EVs affect target tissue in a dose-dependent manner (Tabak et al. 2018). Thus, current studies also indicate that more research on the EV dose-dependent effects should be considered in the future when planning preclinical studies or even clinical trials.

Because motor recovery does not necessarily affect brain tissue regeneration after brain injury and the other way around, the extent of brain tissue injury was measured within the ischemic striatum 84 days after stroke. An increase in neuronal density was found in mice treated with either medium dosage of MSC-EVs or NPC-EVs, suggesting decreased nervous system damage (**Figure 6.A**). Conclusively, medium dosage of NPC-EVs and MSC-EVs thus reduced brain injury on both the morphological and the functional level. Of note, NPC-EVs appear to be not inferior to MSC-EVs, and the medium dosage can achieve the best effects among these three concentrations. This suggest that the dosage of EVs may be one of the key factors for EV-induced neuroprotection independent of the cell source.

Enhanced neurological recovery in the EV groups, however, may not only be contributed to neuroprotection but could also be attributed to neuroregeneration by stimulating endogenous neurogenesis. As we expected, the number of BrdU positive cells was significantly increased in mice treated with the medium dosage of NPC-EVs or MSC-EVs, suggesting increased

proliferation indices (**Figure 6.B**). A differentiation analysis of these newborn BrdU positive cells revealed that NPC-EV or MSC-EV application increases the percentage of BrdU positive cells displaying a neuronal phenotype, as indicated by co-expression of the mature neuronal marker NeuN (**Figure 6.C**). The lack of BrdU and DCX double-positive cells was mainly due to the maturation of newborn neurons from the NPC after 84 days (**Figure 6.D**). This also accounted for the higher number of NeuN and BrdU double-positive cells in the NPC-EV-treated group compared to the control group. The reason for these results may be that NPC-EVs protected neurons after ischemia-reperfusion and promoted the migration and differentiation of NSCs. However, the NPC-EV or MSC-EV high dose group was inferior to the NPC-EV or MSC-EV medium-dose group.

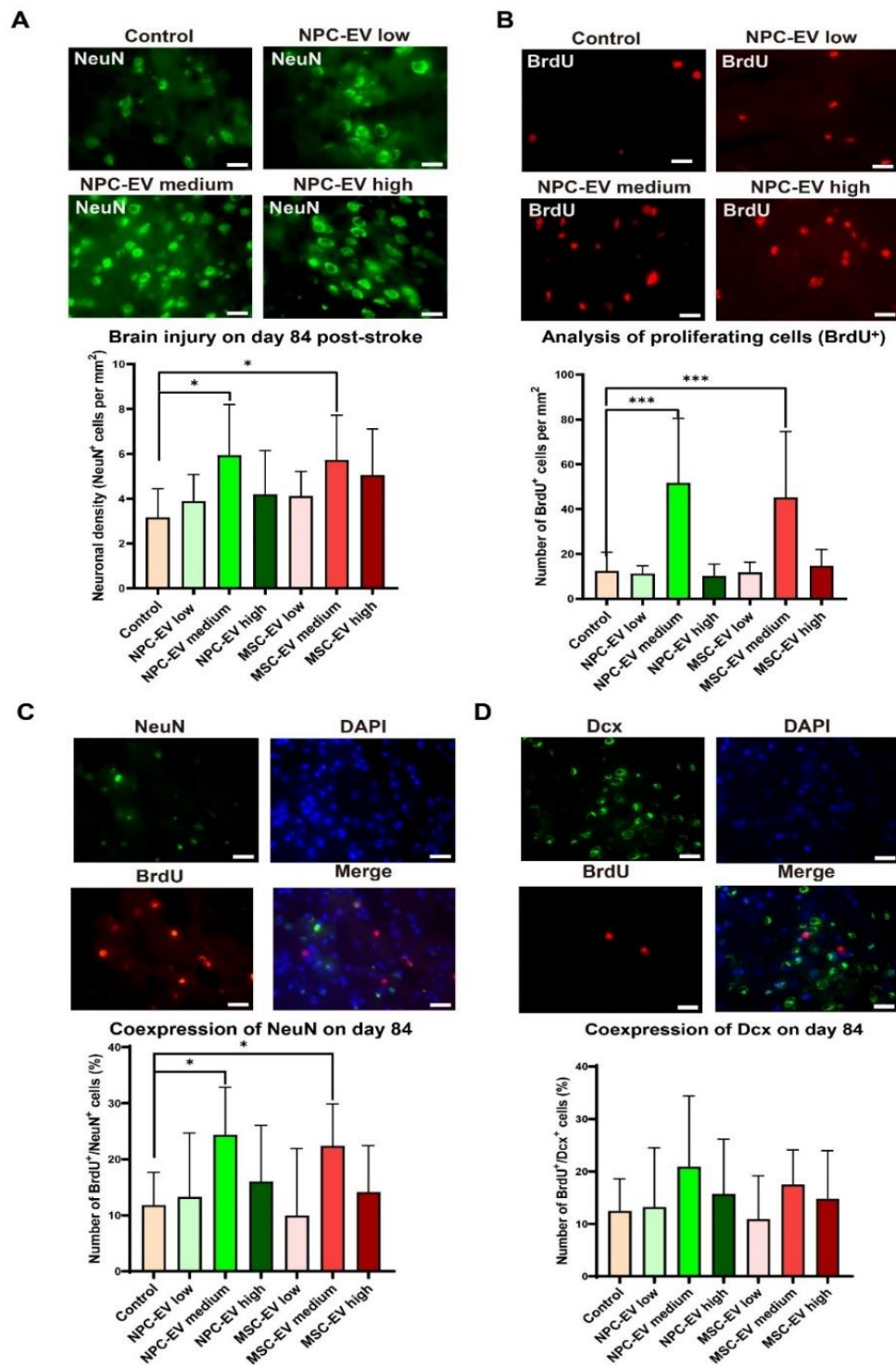


Figure 6. NPC-EVs induce long-term neuroprotection and increase cell proliferation after stroke. **A.** NeuN immunofluorescence staining at day 84 after EV administration showed that the medium EV concentration group stimulated more mature neurogenesis than other EV groups. **B.** BrdU immunofluorescence staining at day 84 showing that NPC-EV or MSC-EV administration stimulates cell proliferation. The medium concentration of EVs showed significant improvement of cell proliferation, while other concentrations did not. **C.** Coexpression of BrdU and NeuN for the detection of newborn neurons after EV administration.

Only the medium concentration group showed a significant improvement of newborn neurons compared to the control group. **D.** Co-expression of BrdU and Dcx for showing the newborn unmaturing neurons after EV administration. No significance was observed in all EV groups compared to the control group. Scale bars: 20 μm . *: $p < 0.05$. Abbreviations: BrdU, 5-Bromo-2-deoxyuridine; DAPI, 4',6-diamidino-2-phenylindole; Dcx, doublecortin; EV, extracellular vesicles; MSC, mesenchymal stem cells; NPC, neural progenitor cell; PBS, phosphate-buffered saline.

Neuronal regeneration does not only imply neurogenesis but also includes complex phenomena such as axonal plasticity. Contralateral stereotactic injection of the anterograde tract tracer BDA into the intact cortex was done to study the degree of axonal plasticity in the poststroke brain. Again, delivery of medium doses of NPC-EVs but not high or low doses showed significantly enhanced axonal plasticity (**Figure 7**). Combining the evidence above, the medium dosage of NPC-EVs or MSC-EVs can achieve the best neuroprotection, neurogenesis, and functional recovery effects in the MCAO model compared to other dosages. The high dosage did not achieve a better effect than the medium dosage, suggesting the effect of EV did not increase with increasing dose. This may be due to the high dosage leading to embolism, reducing the effects. In order to address whether or not EVs directly or indirectly affect the stroke lesion Dil staining and flow cytometry were used to investigate the biodistribution of EVs and the effects of EVs on peripheral organs.

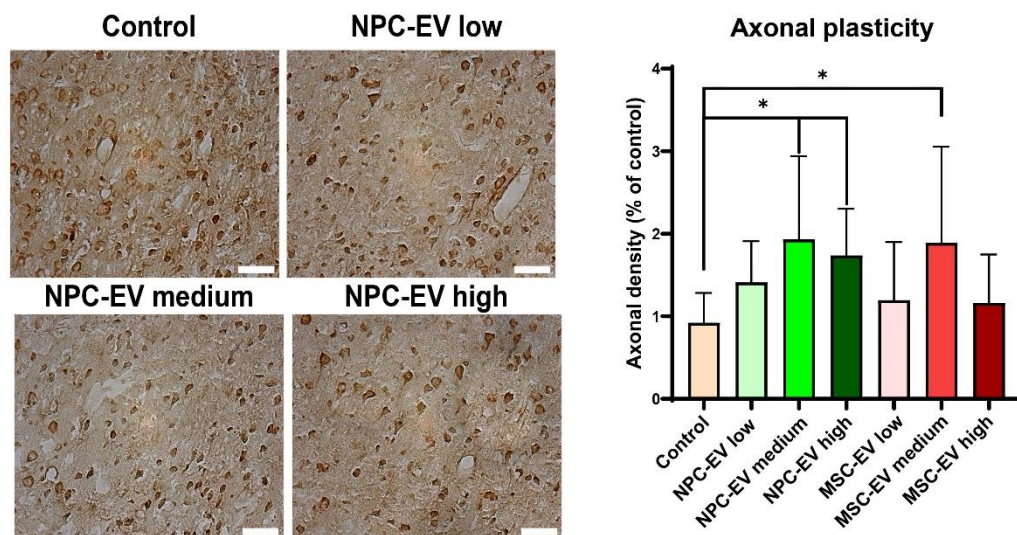


Figure 7. NPC-EV delivery affects post-ischemic axonal plasticity. BDA immunochemistry staining and quantification of axonal recovery after EV administration. NPC-EV medium and high concentration groups enhanced the axonal recovery. Scale bars: 20 μm . *: $p < 0.05$ compare to the control group. Abbreviations: EV, extracellular vesicles; MSC, mesenchymal stem cells; NPC, neural progenitor cell; PBS, phosphate-buffered saline.

4.4 NPC-EVs predominantly distribute in peripheral organs and reverse peripheral poststroke immunosuppression

Systemic transplantation of stem cells is associated with a low number of grafted cells reaching the ischemic brain at all. Rather, these cells are trapped within peripheral organs such as the lung and the spleen (Eggenhofer et al. 2014). Even though EVs are known to cross the BBB (Zagrean et al. 2018), the fact that EVs mainly regulate the peripheral rather than the central immune system (Doepfner et al. 2015b) may indicate that the majority of NPC-EVs does not reach the brain. Indeed, even various systemic delivery routes might affect the distribution patterns of EVs. Therefore, I compared two methods of systemic drug delivery, i.e., retroorbital injection and the femoral vein injection, under both ischemic and non-ischemic conditions. Although NPC-EVs were found both in the brain and in peripheral organs, the majority of EVs were found in the liver and the lung (**Figure 8**). Interestingly, the different delivery routes did not significantly affect the distribution of NPC-EVs. Taking into account the biodistribution patterns of such injected NPC-EVs, the impact of EVs on stroke outcome is multifactorial with some effects being a direct consequence of EV and brain tissue interaction. Since the majority of NPC-EVs is trapped in the periphery, other mechanisms such as the regulation of the peripheral immune response have also been taken into consideration.

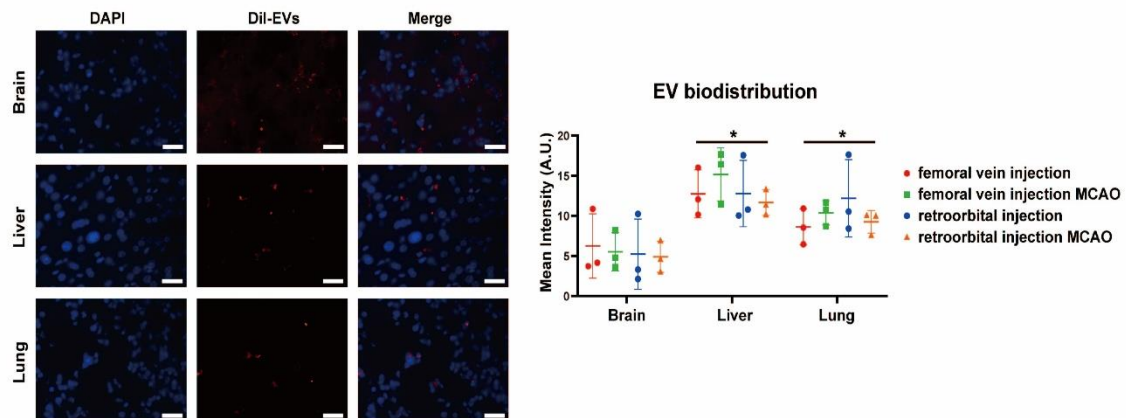


Figure 8. Representative immunofluorescence images displaying the biodistribution of EVs in various organs under different delivery routes and conditions (femoral vein injection, femoral vein injection after MCAO, retroorbital injection, and retroorbital injection after MCAO, $n=3$ animals per group). EVs medium dosage (EVs equivalent to 2×10^6 NPCs) was chosen for the injection. The organs selected for qualitative and quantitative analyses included the brain, liver, and lung (red color shows the DiI marker for EV detection). Most EVs were found in the liver and in the lung. However, the NPC-EV biodistribution patterns showed no differences between the liver and the lung. Different delivery routes and conditions also did not affect the biodistribution of NPC-EVs in peripheral organs. Pictures refer to the femoral vein injection route. Scale bars: 200 μm . Data are shown as mean \pm S.D; *, $p < 0.05$, compare to the brain, $p < 0.05$. Abbreviations: CNS, central nervous system; EV, extracellular vesicle; NPC, neural progenitor cell.

The pathophysiology of cerebral ischemia involves a series of complex inflammatory signaling cascades, which significantly contributes to cell injury (Xing et al. 2012). Previous work on MSC-EVs revealed that MSC-EVs do not affect the central nervous system immune response significantly, but rather reverse peripheral immunosuppression due to stroke itself (Doepfner et al. 2015b). NPC-EVs used herein cause similar effects. Consequently, NPC-EV treatment of mice with either dosage did not affect leukocytes, monocytes, B cells, or T cells in the central nervous system (**Figure 9.A, B, C, D**). Contrarily, flow cytometric analysis of the peripheral blood showed increased B and T lymphocyte numbers in mice treated with the medium dosage of NPC-EVs, but not in mice treated with either high or low doses (**Figure 9.E, F, G, H**). This

observation does not only significantly contribute to brain recovery but may also be immediately relevant under clinical settings by reducing infection risks in stroke patients (Shi et al. 2018). However, one thing that needs to be mentioned is that the neuroprotective effects of NPC-EVs or MSC EVs are more significant in an animal model than in an organoid model. Combining the evidence of the FACS results and the fact that organoids do not contain any immune competent cells, one can suggest that the neuroprotective effects of NPC-EVs are mainly achieved by affecting the peripheral organs, especially the peripheral immune system. The FACS data indicated the increased number of T and B cells in the blood but not in the CNS (**Figure 9**). The pathway analyses based on the proteomic result of NPC-EVs also indicated that the T cell and B cell proliferation regulation and subtype differentiation pathways could be affected by NPC-EVs. Increased B cell numbers, as observed herein, may also support neurogenesis and functional recovery as described before (Ortega et al. 2020). Although T cells have gained increasing attention in recent years, the role of B cells must not be neglected. As such, B cell knock down has already been shown to increase infarct volumes about ten years ago (Ren et al. 2011). IL-10 plays a critical role in B cell-mediated neuroregeneration after stroke (Seifert et al. 2018). As such, IL-10 knockout mice do not show an infarct volume decrease even after B cell transplantation (Seifert et al. 2018). EVs contain many cytokines, including IL10 (Fitzgerald et al. 2018), which may support B cells in this respect.

Although increased T cell numbers were observed in the peripheral blood, a detailed analysis of T cell species was not performed as it was beyond the scope of the current work. Given the important role of Treg cells on immune aspects, future studies on NPC-EVs will also have to focus on the impact of NPC-EVs on these cells. It is important to note that studies observed T cell infiltration into the brain to occur even one month after stroke, thus providing a therapeutic target at the chronic stage of the disease (Xie et al. 2019). In view of the increase in the number of peripheral B cells caused by NPC-EVs, these increased numbers of peripheral B cells may

help reduce the level of active T cells in the brain, thereby increasing the impact on nerve regeneration.

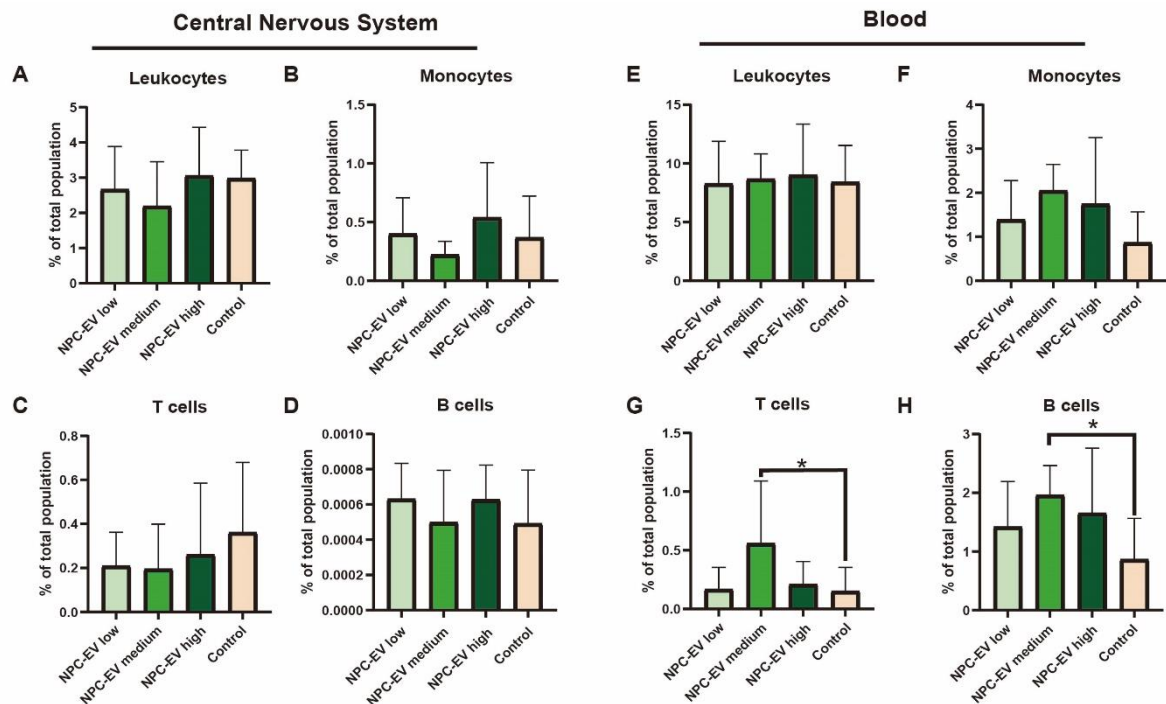


Figure 9. NPC-EVs predominantly distribute in peripheral organs and reverse peripheral poststroke immunosuppression. Mice were subjected to cerebral ischemia for 60 min followed by reperfusion for seven days. The animals (n=5 per condition) received systemic delivery of PBS (control), NPC-EVs low (EVs equivalent to 2×10^5 NPCs), NPC-EVs medium (EVs equivalent to 2×10^6 NPCs), or NPC-EVs high (EVs equivalent to 2×10^7 NPCs) 24 h, 72 h and 120 h post-stroke. Flow cytometry was analyzed with FlowJo software. **A-D.** show the quantitative analysis from CNS samples for **A.** CD45+ CD45int-, **B.** CD11b+, **C.** CD3+, and **D.** CD19+ cells. In **E-H.**, the quantitative analyses from blood samples for **E.** CD45+ Cd45int-, **F.** CD11b+, **G.** CD3+, and **H.** CD19+ cells are given. NPC-EV medium increased both T cell and B cell populations in the peripheral blood but did not affect the CNS. Scale bars: 20 μ m. *: p<0.05. Abbreviations: EV, extracellular vesicles; MSC, mesenchymal stem cells; NPC, neural progenitor cell; PBS, phosphate-buffered saline.

Flow cytometry results are consistent with previous behavioral and immunofluorescence staining results, showing that the medium dosage could achieve the beneficial effects, but not the low and high dosage in NPC-derived EVs or MSC-derived EVs. The insufficient effects of low dosage may be due to the reduced concentration of EVs that induce these effects. However, the higher dosage of EVs should achieve better effects when compared to the medium dosage,

but the result was opposite. The low effects of the high dosage may be due to embolism formation in the EV high concentration condition. However, embolism formation of EVs should cause pulmonary embolism as most of the EVs were trapped in the lung and liver, but no higher animal death rates were observed in the high EV group. This suggests that the insufficient effects of high dosage EVs may not be caused by the embolism formation but by a hitherto unknown mechanism. We found a small amount of interleukin-1 receptor accessory protein in NPC-EVs, which can stimulate proinflammatory pathways and activate macrophages. In the low and medium dosage, the activation of macrophages by proinflammatory cytokines in EVs is not distinct. However, in the high dosage, the proinflammatory cytokines in EVs reach a level that stimulates macrophage activation. These activated macrophages degrade the majority of systemically administered EVs, resulting in a lower number of functional EVs *in vivo*. The high dosage of EVs may also stimulate other immune-related pathways that accelerate EV degradation *in vivo*. The impact of NPC-EVs on macrophages or other immune-related pathways needs to be further elucidated, but it was beyond the scope of this thesis. The present data suggests that there is an optimum concentration for stem cell-derived EVs treatment.

In conclusion, our study qualifies SVZ-derived NPC-EVs as practical tools of neuroprotection and neuroregeneration under experimental stroke conditions. An overview of potential mechanisms being involved is summarized in **Figure 10**.

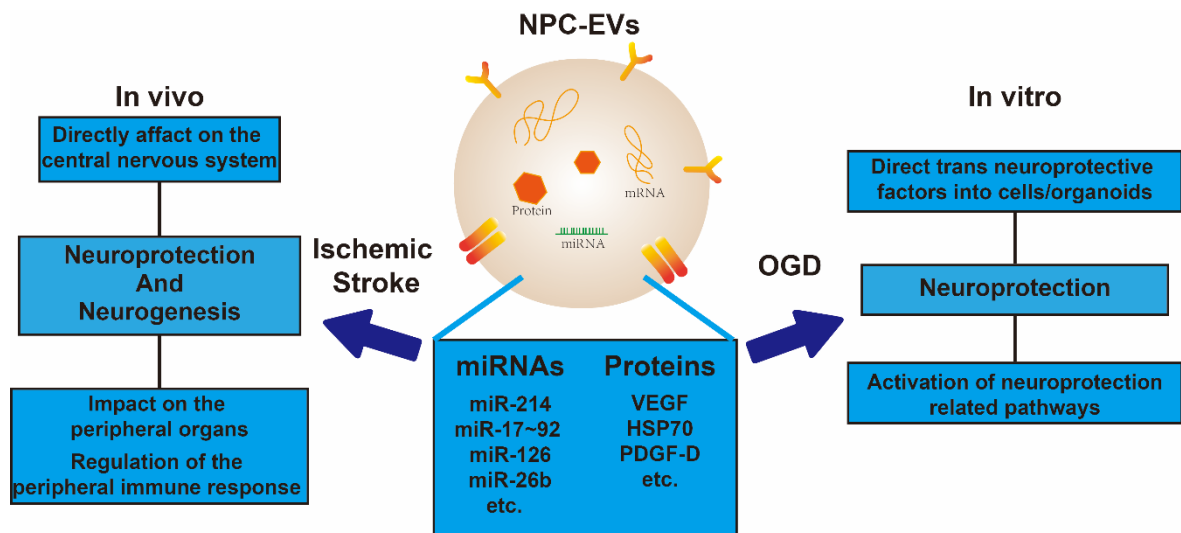


Figure 10. Overview of potential mechanisms being involved in NPC-EV-induced neuroprotection and neurogenesis. NPC-EVs directly transfer neuroprotective factors into target cells or organoids to induce neuroprotective effects *in vitro*. Although NPC-EVs can directly affect the central nervous system *in vivo*, since most NPC-EVs do not reach the brain, the neuroprotective and neurogenesis effects induced by NPC-EVs are mostly indirect. Abbreviations: OGD = oxygen-glucose deprivation; NPC-EV = neural progenitor cell extracellular vesicles; VEGF = vascular endothelial growth factor; HSP70 = 70 kilodalton heat shock protein; PDGF-D = platelet-derived growth factor D.

Due to the heterogeneous cargo of NPC-EVs, the underlying mechanisms are pleiotropic and intricate, and fully elucidating these mechanisms was beyond the aim of this thesis. However, the translation potential of EVs is highly promising, overcoming the disadvantages of stem cell transplants. After extensive negative clinical trials on neuroprotective drugs, EVs may therefore change modern stroke treatment in the future.

5 References

- Abels ER, Breakefield XO (2016): Introduction to Extracellular Vesicles: Biogenesis, RNA Cargo Selection, Content, Release, and Uptake. *Cell Mol Neurobiol* 36, 301-312
- Bacigaluppi M, Pluchino S, Peruzzotti-Jametti L, Kilic E, Kilic U, Salani G, Brambilla E, West MJ, Comi G, Martino G, et al. (2009): Delayed post-ischaemic neuroprotection following systemic neural stem cell transplantation involves multiple mechanisms. *Brain* 132, 2239-2251
- Bernstock JD, Peruzzotti-Jametti L, Ye D, Gessler FA, Maric D, Vicario N, Lee YJ, Pluchino S, Hallenbeck JM (2017): Neural stem cell transplantation in ischemic stroke: A role for preconditioning and cellular engineering. *J Cereb Blood Flow Metab* 37, 2314-2319
- Boehme AK, Esenwa C, Elkind MS (2017): Stroke Risk Factors, Genetics, and Prevention. *Circ Res* 120, 472-495
- Borlongan CV (2019): Concise Review: Stem Cell Therapy for Stroke Patients: Are We There Yet? *Stem Cells Transl Med* 8, 983-988
- Buschmann D, Kirchner B, Hermann S, Marte M, Wurmser C, Brandes F, Kotschote S, Bonin M, Steinlein OK, Pfaffl MW, et al. (2018): Evaluation of serum extracellular vesicle isolation methods for profiling miRNAs by next-generation sequencing. *J Extracell Vesicles* 7, 1481321
- Carpintero-Fernandez P, Fafian-Labora J, O'Loughlen A (2017): Technical Advances to Study Extracellular Vesicles. *Front Mol Biosci* 4, 79
- Chan SJ, Niu W, Hayakawa K, Hamanaka G, Wang X, Cheah PS, Guo S, Yu Z, Arai K, Selim MH, et al. (2019): Promoting Neuro-Supportive Properties of Astrocytes with Epidermal Growth Factor Hydrogels. *Stem Cells Transl Med* 8, 1242-1248
- Chrostek MR, Fellows EG, Crane AT, Grande AW, Low WC (2019): Efficacy of stem cell-based therapies for stroke. *Brain Res* 1722, 146362
- Dayer AG, Ford AA, Cleaver KM, Yassaee M, Cameron HA (2003): Short-term and long-term survival of new neurons in the rat dentate gyrus. *J Comp Neurol* 460, 563-572
- Doepfner TR, Kaltwasser B, Bahr M, Hermann DM (2014): Effects of neural progenitor cells on post-stroke neurological impairment-a detailed and comprehensive analysis of behavioral tests. *Front Cell Neurosci* 8, 338
- Doepfner TR, Kaltwasser B, Fengyan J, Hermann DM, Bahr M (2013a): TAT-Hsp70 induces neuroprotection against stroke via anti-inflammatory actions providing appropriate cellular microenvironment for transplantation of neural precursor cells. *J Cereb Blood Flow Metab* 33, 1778-1788
- Doepfner TR, El Aanbouri M, Dietz GP, Weise J, Schwarting S, Bahr M (2010): Transplantation of TAT-Bcl-xL-transduced neural precursor cells: long-term neuroprotection after stroke. *Neurobiol Dis* 40, 265-276
- Doepfner TR, Nagel F, Dietz GP, Weise J, Tonges L, Schwarting S, Bahr M (2009): TAT-Hsp70-mediated neuroprotection and increased survival of neuronal precursor cells after focal cerebral ischemia in mice. *J Cereb Blood Flow Metab* 29, 1187-1196

- Doepfner TR, Kaltwasser B, Teli MK, Sanchez-Mendoza EH, Kilic E, Bahr M, Hermann DM (2015a): Post-stroke transplantation of adult subventricular zone derived neural progenitor cells--A comprehensive analysis of cell delivery routes and their underlying mechanisms. *Exp Neurol* 273, 45-56
- Doepfner TR, Traut V, Heidenreich A, Kaltwasser B, Bosche B, Bahr M, Hermann DM (2017a): Conditioned Medium Derived from Neural Progenitor Cells Induces Long-term Post-ischemic Neuroprotection, Sustained Neurological Recovery, Neurogenesis, and Angiogenesis. *Mol Neurobiol* 54, 1531-1540
- Doepfner TR, Doehring M, Kaltwasser B, Majid A, Lin F, Bahr M, Kilic E, Hermann DM (2017b): Ischemic Post-Conditioning Induces Post-Stroke Neuroprotection via Hsp70-Mediated Proteasome Inhibition and Facilitates Neural Progenitor Cell Transplantation. *Mol Neurobiol* 54, 6061-6073
- Doepfner TR, Bretschneider E, Doehring M, Segura I, Senturk A, Acker-Palmer A, Hasan MR, Elali A, Hermann DM, Bahr M (2011): Enhancement of endogenous neurogenesis in ephrin-B3 deficient mice after transient focal cerebral ischemia. *Acta neuropathologica* 122, 429-442
- Doepfner TR, Doehring M, Bretschneider E, Zechariah A, Kaltwasser B, Muller B, Koch JC, Bahr M, Hermann DM, Michel U (2013b): MicroRNA-124 protects against focal cerebral ischemia via mechanisms involving Usp14-dependent REST degradation. *Acta neuropathologica* 126, 251-265
- Doepfner TR, Herz J, Gorgens A, Schlechter J, Ludwig AK, Radtke S, de Miroschedji K, Horn PA, Giebel B, Hermann DM (2015b): Extracellular Vesicles Improve Post-Stroke Neuroregeneration and Prevent Postischemic Immunosuppression. *Stem Cells Transl Med* 4, 1131-1143
- Doepfner TR, Ewert TA, Tonges L, Herz J, Zechariah A, Elali A, Ludwig AK, Giebel B, Nagel F, Dietz GP, et al. (2012): Transduction of Neural Precursor Cells with TAT-Heat Shock Protein 70 Chaperone: Therapeutic Potential Against Ischemic Stroke after Intrastratial and Systemic Transplantation. *Stem Cells* 30, 1297-1310
- Doetsch F, Caille I, Lim DA, Garcia-Verdugo JM, Alvarez-Buylla A (1999): Subventricular zone astrocytes are neural stem cells in the adult mammalian brain. *Cell* 97, 703-716
- Doyle LM, Wang MZ (2019): Overview of Extracellular Vesicles, Their Origin, Composition, Purpose, and Methods for Exosome Isolation and Analysis. *Cells* 8
- Egashira Y, Sugitani S, Suzuki Y, Mishiro K, Tsuruma K, Shimazawa M, Yoshimura S, Iwama T, Hara H (2012): The conditioned medium of murine and human adipose-derived stem cells exerts neuroprotective effects against experimental stroke model. *Brain Res* 1461, 87-95
- Eggenhofer E, Luk F, Dahlke MH, Hoogduijn MJ (2014): The life and fate of mesenchymal stem cells. *Front Immunol* 5, 148
- Fitzgerald W, Freeman ML, Lederman MM, Vasilieva E, Romero R, Margolis L (2018): A System of Cytokines Encapsulated in ExtraCellular Vesicles. *Sci Rep* 8, 8973

- Gatti S, Bruno S, Deregibus MC, Sordi A, Cantaluppi V, Tetta C, Camussi G (2011): Microvesicles derived from human adult mesenchymal stem cells protect against ischaemia-reperfusion-induced acute and chronic kidney injury. *Nephrology, dialysis, transplantation : official publication of the European Dialysis and Transplant Association - European Renal Association* 26, 1474-1483
- Giffard RG, Yenari MA (2004): Many mechanisms for hsp70 protection from cerebral ischemia. *J Neurosurg Anesthesiol* 16, 53-61
- Gladstone DJ, Black SE, Hakim AM, Heart, Stroke Foundation of Ontario Centre of Excellence in Stroke R (2002): Toward wisdom from failure: lessons from neuroprotective stroke trials and new therapeutic directions. *Stroke* 33, 2123-2136
- Gu N, Rao C, Tian Y, Di Z, Liu Z, Chang M, Lei H (2014): Anti-inflammatory and antiapoptotic effects of mesenchymal stem cells transplantation in rat brain with cerebral ischemia. *J Stroke Cerebrovasc Dis* 23, 2598-2606
- Guo W, Patzlaff NE, Jobe EM, Zhao X (2012): Isolation of multipotent neural stem or progenitor cells from both the dentate gyrus and subventricular zone of a single adult mouse. *Nat Protoc* 7, 2005-2012
- Hamzei Taj S, Kho W, Riou A, Wiedermann D, Hoehn M (2016): MiRNA-124 induces neuroprotection and functional improvement after focal cerebral ischemia. *Biomaterials* 91, 151-165
- Harder S, Klinkhardt U (2000): Thrombolytics: drug interactions of clinical significance. *Drug Saf* 23, 391-399
- Harrell CR, Jovicic N, Djonov V, Arsenijevic N, Volarevic V (2019): Mesenchymal Stem Cell-Derived Exosomes and Other Extracellular Vesicles as New Remedies in the Therapy of Inflammatory Diseases. *Cells* 8
- Hill AF (2019): Extracellular Vesicles and Neurodegenerative Diseases. *J Neurosci* 39, 9269-9273
- Huang P, Gebhart N, Richelson E, Brott TG, Meschia JF, Zubair AC (2014): Mechanism of mesenchymal stem cell-induced neuron recovery and anti-inflammation. *Cytotherapy* 16, 1336-1344
- Jiang Y, He R, Shi Y, Liang J, Zhao L (2020): Plasma exosomes protect against cerebral ischemia/reperfusion injury via exosomal HSP70 mediated suppression of ROS. *Life Sci* 256, 117987
- Jin J, Ko H, Sun T, Kim SN (2018): Distinct function of miR-17-92 cluster in the dorsal and ventral adult hippocampal neurogenesis. *Biochem Biophys Res Commun* 503, 1594-1598
- Jin K, Wang X, Xie L, Mao XO, Zhu W, Wang Y, Shen J, Mao Y, Banwait S, Greenberg DA (2006): Evidence for stroke-induced neurogenesis in the human brain. *Proc Natl Acad Sci U S A* 103, 13198-13202
- Joers VL, Emborg ME (2009): Preclinical assessment of stem cell therapies for neurological diseases. *ILAR J* 51, 24-41

- Kaneko N, Kako E, Sawamoto K (2011): Prospects and limitations of using endogenous neural stem cells for brain regeneration. *Genes (Basel)* 2, 107-130
- Kempermann G, Gast D, Kronenberg G, Yamaguchi M, Gage FH (2003): Early determination and long-term persistence of adult-generated new neurons in the hippocampus of mice. *Development* 130, 391-399
- Keshtkar S, Azarpira N, Ghahremani MH (2018): Mesenchymal stem cell-derived extracellular vesicles: novel frontiers in regenerative medicine. *Stem Cell Res Ther* 9, 63
- Kubo H (2018): Extracellular Vesicles in Lung Disease. *Chest* 153, 210-216
- Lai RC, Arslan F, Lee MM, Sze NS, Choo A, Chen TS, Salto-Tellez M, Timmers L, Lee CN, El Oakley RM, et al. (2010): Exosome secreted by MSC reduces myocardial ischemia/reperfusion injury. *Stem Cell Res* 4, 214-222
- Li C, Cheung MKH, Han S, Zhang Z, Chen L, Chen J, Zeng H, Qiu J (2019): Mesenchymal stem cells and their mitochondrial transfer: a double-edged sword. *Biosci Rep* 39
- Liu G, David BT, Trawczynski M, Fessler RG (2020): Advances in Pluripotent Stem Cells: History, Mechanisms, Technologies, and Applications. *Stem Cell Rev Rep* 16, 3-32
- Lobb RJ, Becker M, Wen SW, Wong CS, Wiegman AP, Leimgruber A, Moller A (2015): Optimized exosome isolation protocol for cell culture supernatant and human plasma. *J Extracell Vesicles* 4, 27031
- Ludwig AK, De Miroschedji K, Doeppner TR, Borger V, Ruesing J, Rebmann V, Durst S, Jansen S, Bremer M, Behrmann E, et al. (2018): Precipitation with polyethylene glycol followed by washing and pelleting by ultracentrifugation enriches extracellular vesicles from tissue culture supernatants in small and large scales. *J Extracell Vesicles* 7, 1528109
- Ma S, Zhong D, Chen H, Zheng Y, Sun Y, Luo J, Li H, Li G, Yin Y (2013): The immunomodulatory effect of bone marrow stromal cells (BMSCs) on interleukin (IL)-23/IL-17-mediated ischemic stroke in mice. *J Neuroimmunol* 257, 28-35
- Marti-Fabregas J, Romaguera-Ros M, Gomez-Pinedo U, Martinez-Ramirez S, Jimenez-Xarrie E, Marin R, Marti-Vilalta JL, Garcia-Verdugo JM (2010): Proliferation in the human ipsilateral subventricular zone after ischemic stroke. *Neurology* 74, 357-365
- Matsuoka H, Tamura A, Kinehara M, Shima A, Uda A, Tahara H, Michihara A (2018): Levels of tight junction protein CLDN1 are regulated by microRNA-124 in the cerebellum of stroke-prone spontaneously hypertensive rats. *Biochem Biophys Res Commun* 498, 817-823
- Motamed S, Del Borgo MP, Zhou K, Kulkarni K, Crack PJ, Merson TD, Aguilar MI, Finkelstein DI, Forsythe JS (2019): Migration and Differentiation of Neural Stem Cells Diverted From the Subventricular Zone by an Injectable Self-Assembling beta-Peptide Hydrogel. *Front Bioeng Biotechnol* 7, 315
- Musuka TD, Wilton SB, Traboulsi M, Hill MD (2015): Diagnosis and management of acute ischemic stroke: speed is critical. *CMAJ* 187, 887-893

- Nakai W, Yoshida T, Diez D, Miyatake Y, Nishibu T, Imawaka N, Naruse K, Sadamura Y, Hanayama R (2016): A novel affinity-based method for the isolation of highly purified extracellular vesicles. *Sci Rep* 6, 33935
- Ophelders DR, Wolfs TG, Jellema RK, Zwanenburg A, Andriessen P, Delhaas T, Ludwig AK, Radtke S, Peters V, Janssen L, et al. (2016): Mesenchymal Stromal Cell-Derived Extracellular Vesicles Protect the Fetal Brain After Hypoxia-Ischemia. *Stem Cells Transl Med* 5, 754-763
- Ortega SB, Torres VO, Latchney SE, Whoolery CW, Noorbhai IZ, Poinsette K, Selvaraj UM, Benson MA, Meeuwissen AJM, Plautz EJ, et al. (2020): B cells migrate into remote brain areas and support neurogenesis and functional recovery after focal stroke in mice. *Proc Natl Acad Sci U S A* 117, 4983-4993
- Pan WL, Chopp M, Fan B, Zhang R, Wang X, Hu J, Zhang XM, Zhang ZG, Liu XS (2019): Ablation of the microRNA-17-92 cluster in neural stem cells diminishes adult hippocampal neurogenesis and cognitive function. *FASEB J* 33, 5257-5267
- Reisman M, Adams KT (2014): Stem cell therapy: a look at current research, regulations, and remaining hurdles. *P T* 39, 846-857
- Ren X, Akiyoshi K, Dziennis S, Vandenbark AA, Herson PS, Hurn PD, Offner H (2011): Regulatory B cells limit CNS inflammation and neurologic deficits in murine experimental stroke. *J Neurosci* 31, 8556-8563
- Rumajogee P, Altamentova S, Li L, Li J, Wang J, Kuurstra A, Khazaei M, Beldick S, Menon RS, van der Kooy D, et al. (2018): Exogenous Neural Precursor Cell Transplantation Results in Structural and Functional Recovery in a Hypoxic-Ischemic Hemiplegic Mouse Model. *eNeuro* 5
- Saraiva C, Talhada D, Rai A, Ferreira R, Ferreira L, Bernardino L, Ruscher K (2018): MicroRNA-124-loaded nanoparticles increase survival and neuronal differentiation of neural stem cells in vitro but do not contribute to stroke outcome in vivo. *PLoS One* 13, e0193609
- Schaar KL, Brenneman MM, Savitz SI (2010): Functional assessments in the rodent stroke model. *Experimental & translational stroke medicine* 2, 13
- Seifert HA, Vandenbark AA, Offner H (2018): Regulatory B cells in experimental stroke. *Immunology* 154, 169-177
- Seitz RJ (2016): The pros and cons of intravenous thrombolysis in stroke. *Lancet Neurol* 15, 997-998
- Shi K, Wood K, Shi FD, Wang X, Liu Q (2018): Stroke-induced immunosuppression and poststroke infection. *Stroke Vasc Neurol* 3, 34-41
- Singh M, Pandey PK, Bhasin A, Padma MV, Mohanty S (2020): Application of Stem Cells in Stroke: A Multifactorial Approach. *Front Neurosci* 14, 473
- Starke RM, Turk A, Ding D, Crowley RW, Liu KC, Chalouhi N, Hasan DM, Dumont AS, Jabbour P, Durst CR, et al. (2016): Technology developments in endovascular treatment of intracranial aneurysms. *J Neurointerv Surg* 8, 135-144

- Tabak S, Schreiber-Avissar S, Beit-Yannai E (2018): Extracellular vesicles have variable dose-dependent effects on cultured draining cells in the eye. *J Cell Mol Med* 22, 1992-2000
- Tang G, Liu Y, Zhang Z, Lu Y, Wang Y, Huang J, Li Y, Chen X, Gu X, Wang Y, et al. (2014): Mesenchymal stem cells maintain blood-brain barrier integrity by inhibiting aquaporin-4 upregulation after cerebral ischemia. *Stem Cells* 32, 3150-3162
- Tang Z, Arjunan P, Lee C, Li Y, Kumar A, Hou X, Wang B, Wardega P, Zhang F, Dong L, et al. (2010): Survival effect of PDGF-CC rescues neurons from apoptosis in both brain and retina by regulating GSK3beta phosphorylation. *J Exp Med* 207, 867-880
- Thery C, Amigorena S, Raposo G, Clayton A (2006): Isolation and characterization of exosomes from cell culture supernatants and biological fluids. *Curr Protoc Cell Biol* Chapter 3, Unit 3 22
- Thery C, Witwer KW, Aikawa E, Alcaraz MJ, Anderson JD, Andriantsitohaina R, Antoniou A, Arab T, Archer F, Atkin-Smith GK, et al. (2018): Minimal information for studies of extracellular vesicles 2018 (MISEV2018): a position statement of the International Society for Extracellular Vesicles and update of the MISEV2014 guidelines. *J Extracell Vesicles* 7, 1535750
- Wang HZ, Yang C, Zhang BY, Li N, Han Z, Chen F (2019): Influence of mesenchymal stem cells on respiratory distress syndrome in newborn swines via the JAK-STAT signaling pathway. *Eur Rev Med Pharmacol Sci* 23, 7550-7556
- Wang Y, Kilic E, Kilic U, Weber B, Bassetti CL, Marti HH, Hermann DM (2005): VEGF overexpression induces post-ischaemic neuroprotection, but facilitates haemodynamic steal phenomena. *Brain* 128, 52-63
- Wilcox JT, Satkunendrarajah K, Zuccato JA, Nassiri F, Fehlings MG (2014): Neural precursor cell transplantation enhances functional recovery and reduces astrogliosis in bilateral compressive/contusive cervical spinal cord injury. *Stem Cells Transl Med* 3, 1148-1159
- Xie L, Li W, Hersh J, Liu R, Yang SH (2019): Experimental ischemic stroke induces long-term T cell activation in the brain. *J Cereb Blood Flow Metab* 39, 2268-2276
- Xin H, Li Y, Cui Y, Yang JJ, Zhang ZG, Chopp M (2013): Systemic administration of exosomes released from mesenchymal stromal cells promote functional recovery and neurovascular plasticity after stroke in rats. *Journal of cerebral blood flow and metabolism : official journal of the International Society of Cerebral Blood Flow and Metabolism* 33, 1711-1715
- Xing C, Arai K, Lo EH, Hommel M (2012): Pathophysiologic cascades in ischemic stroke. *Int J Stroke* 7, 378-385
- Yamashita T, Ninomiya M, Hernandez Acosta P, Garcia-Verdugo JM, Sunabori T, Sakaguchi M, Adachi K, Kojima T, Hirota Y, Kawase T, et al. (2006): Subventricular zone-derived neuroblasts migrate and differentiate into mature neurons in the post-stroke adult striatum. *J Neurosci* 26, 6627-6636

- Yang H, Wang C, Chen H, Li L, Ma S, Wang H, Fu Y, Qu T (2018): Neural Stem Cell-Conditioned Medium Ameliorated Cerebral Ischemia-Reperfusion Injury in Rats. *Stem Cells Int* 2018, 4659159
- Yang J, Zhang X, Chen X, Wang L, Yang G (2017): Exosome Mediated Delivery of miR-124 Promotes Neurogenesis after Ischemia. *Molecular therapy. Nucleic acids* 7, 278-287
- Yang P, Cai L, Zhang G, Bian Z, Han G (2017): The role of the miR-17-92 cluster in neurogenesis and angiogenesis in the central nervous system of adults. *J Neurosci Res* 95, 1574-1581
- Zagrean AM, Hermann DM, Opris I, Zagrean L, Popa-Wagner A (2018): Multicellular Crosstalk Between Exosomes and the Neurovascular Unit After Cerebral Ischemia. Therapeutic Implications. *Front Neurosci* 12, 811
- Zhang GL, Zhu ZH, Wang YZ (2019): Neural stem cell transplantation therapy for brain ischemic stroke: Review and perspectives. *World J Stem Cells* 11, 817-830
- Zhang P, Li J, Liu Y, Chen X, Lu H, Kang Q, Li W, Gao M (2011): Human embryonic neural stem cell transplantation increases subventricular zone cell proliferation and promotes peri-infarct angiogenesis after focal cerebral ischemia. *Neuropathology : official journal of the Japanese Society of Neuropathology* 31, 384-391
- Zhang Y, Chopp M, Liu XS, Katakowski M, Wang X, Tian X, Wu D, Zhang ZG (2017): Exosomes Derived from Mesenchymal Stromal Cells Promote Axonal Growth of Cortical Neurons. *Mol Neurobiol* 54, 2659-2673
- Zhu J, Liu Q, Jiang Y, Wu L, Xu G, Liu X (2015): Enhanced angiogenesis promoted by human umbilical mesenchymal stem cell transplantation in stroked mouse is Notch1 signaling associated. *Neuroscience* 290, 288-299

6 Copy of the Publication 1

Translational Stroke Research (2021) 12:185–203
<https://doi.org/10.1007/s12975-020-00814-z>

ORIGINAL ARTICLE



Extracellular Vesicles Derived from Neural Progenitor Cells—a Preclinical Evaluation for Stroke Treatment in Mice

X. Zheng¹ · L. Zhang¹ · Y. Kuang¹ · V. Venkataramani² · F. Jin³ · K. Hein¹ · M. P. Zafeiriou^{4,5,6} · C. Lenz^{7,8} · W. Moebius⁹ · E. Kilic¹⁰ · D. M. Hermann¹¹ · M. S. Weber^{1,12} · H. Urlaub^{7,8} · W.-H. Zimmermann^{4,5,6} · M. Bähr¹ · Thorsten R. Doepfner^{1,10}

Received: 10 October 2019 / Revised: 30 March 2020 / Accepted: 6 April 2020 / Published online: 2 May 2020
 © The Author(s) 2020

Abstract

Stem cells such as mesenchymal stem cells (MSCs) enhance neurological recovery in preclinical stroke models by secreting extracellular vesicles (EVs). Since previous reports have focused on the application of MSC-EVs only, the role of the most suitable host cell for EV enrichment and preclinical stroke treatment remains elusive. The present study aimed to evaluate the therapeutic potential of EVs derived from neural progenitor cells (NPCs) following experimental stroke. Using the PEG technique, EVs were enriched and characterized by electron microscopy, proteomics, rt-PCR, nanosight tracking analysis, and Western blotting. Different dosages of NPC-EVs displaying a characteristic profile in size, shape, cargo protein, and non-coding RNA contents were incubated in the presence of cerebral organoids exposed to oxygen-glucose deprivation (OGD), significantly reducing cell injury when compared with control organoids. Systemic administration of NPC-EVs in male C57BL6 mice following experimental ischemia enhanced neurological recovery and neuroregeneration for as long as 3 months. Interestingly, the therapeutic impact of such NPC-EVs was found to be not inferior to MSC-EVs. Flow cytometric analyses of blood and brain samples 7 days post-stroke demonstrated increased blood concentrations of B and T lymphocytes after NPC-EV delivery, without affecting cerebral cell counts. Likewise, a biodistribution analysis after systemic delivery of NPC-EVs revealed the majority of NPC-EVs to be found in extracranial organs such as the liver and the lung. This proof-of-concept study supports the idea of EVs being a general concept of stem cell–induced neuroprotection under stroke conditions, where EVs contribute to reverting the peripheral post-stroke immunosuppression.

Electronic supplementary material The online version of this article (<https://doi.org/10.1007/s12975-020-00814-z>) contains supplementary material, which is available to authorized users.

✉ Thorsten R. Doepfner
 thorsten.doepfner@med.uni-goettingen.de

¹ Department of Neurology, University Medical Center Goettingen, Robert-Koch-Str. 40, 37075 Goettingen, Germany

² Institute of Pathology, University Medical Center Goettingen, Goettingen, Germany

³ Department of Hematology, Cancer Center, The First Hospital of Jilin University, Changchun, Jilin, China

⁴ Institute for Pharmacology and Toxicology, University Medical Center Goettingen, Goettingen, Germany

⁵ DZHK (German Center for Cardiovascular Research), partner site Goettingen, Göttingen, Germany

⁶ Cluster of Excellence “Multiscale Bioimaging: from Molecular Machines to Networks of Excitable Cells” (MBExC), University of Goettingen, Göttingen, Germany

⁷ Bioanalytical Mass Spectrometry Group, Max Planck Institute for Biophysical Chemistry, Goettingen, Germany

⁸ Institute of Clinical Chemistry, Bioanalytics, University Medical Center Goettingen, Goettingen, Germany

⁹ Department of Neurogenetics, Electron Microscopy Group, Max Planck Institute of Experimental Medicine, Goettingen, Germany

¹⁰ Regenerative and Restorative Medical Research Center, Istanbul Medipol University, Istanbul, Turkey

¹¹ Department of Neurology, University of Duisburg-Essen Medical School, Essen, Germany

¹² Institute for Neuropathology, University Medical Center Goettingen, Goettingen, Germany

Keywords Cerebral ischemia · Extracellular vesicles, neural progenitor cells · Neurological recovery · Neuroregeneration

Introduction

The systemic transplantation of stem cells such as mesenchymal stem cells (MSCs) and neural progenitor cells (NPCs) promotes neurological recovery, angiogenesis, and neurogenesis in animal models of cerebral ischemia [1–7]. The majority of these grafted cells, however, are trapped in extracerebral organs and do not integrate into existing neural networks. Rather, transplanted stem cells display both low survival rates and poor differentiation rates within the ischemic milieu [8–11], suggesting an indirect mode of action by which post-stroke neurological recovery is achieved.

It has been demonstrated that stem cell-derived conditioned medium induces similar effects in various disease models when compared with stem cell transplantation itself [12, 13]. MSCs and other cell types secrete neurotrophic factors such as EGF and VEGF, thus inducing both neuroprotection and neuroregeneration [14–16]. Recent research, however, has questioned the hypothesis that these beneficial factors are the sole biological key mediator of stem cell-induced brain protection against cerebral ischemia. Instead, bilayer structured vesicles, termed extracellular vesicles (EVs), secreted from eukaryotic cells, including MSCs, have been found to be critical players in the aforementioned process. These EVs have also been detected in conditioned medium derived from stem cells [17, 18], further supporting the idea that EVs are biological mediators of stem cell-induced actions under conditions of cerebral ischemia.

EVs are a heterogeneous group of vesicles ranging in size from 30 to 1000 nm. They contain a defined set of cargo, which depends on the characteristics of the source cell [19]. EV cargo consists of non-coding RNAs, DNA, and proteins such as heat shock proteins and tetraspanins [20, 21]. Although fundamental questions in the emerging EV field still need to be addressed, the current concept divides EVs into exosomes, microvesicles, and apoptotic bodies. Current stroke research focuses on microvesicles and especially exosomes. Both exosomes and microvesicles are a consequence of direct outward budding or pinching of the plasma membrane, with microvesicles being derivatives of multivesicular bodies (MVB) that bud on the cell surface to be released into the extracellular environment [22]. The present work focuses on further elucidating the therapeutic potential of EVs rather than on distinguishing the various subtypes of EVs. Hence, the term EVs is used throughout the manuscript.

EVs exert a plethora of beneficial therapeutic effects in various disease models such as myocardial ischemia, liver fibrosis, kidney injury, and cerebral ischemia [23–27]. Indeed, previous research from our group and others have

systematically studied the impact of systemic MSC-derived EV infusion on stroke outcome, demonstrating an increased neurological recovery, an enhanced neuroregeneration, and a modified post-stroke immune response upon EV treatment [17, 28, 29]. Whereas the majority of regenerative stroke research focuses on the transplantation of MSCs, therapeutic results were also observed for other cell types such as NPCs [1, 30–32]. On the contrary, the therapeutic potential of subventricular zone-derived NPC-EVs under stroke conditions has not been addressed. Although EVs appear to be an attractive tool for prospective adjuvant stroke treatment, fundamental issues have to be solved, among which is the relevance of the host cell for EV harvest. Therefore, following *in vitro* characterization of enriched NPC-EVs, we evaluated their therapeutic potential in models of both *in vitro* hypoxia and *in vivo* stroke.

Materials and Methods

Primary Culture of MSCs and NPCs

P1 newborn mice were anesthetized using CO₂ euthanasia. The brain was removed, and the subventricular zone (SVZ) was dissected in cold PBS under microscopic control. Tissue chunks were spun down at 200g for 1 min at 4 °C. The supernatant was discarded, and the tissue was incubated with 1 ml of 0.05% trypsin-EDTA in 15-ml conical tubes. The tubes were gently shaken at room temperature (RT) for 15 min. Each cell pellet was resuspended with 5.5 ml of NPC cell culture medium (DMEM F-12 medium, B27 (Thermo Fisher, Waltham, USA), L-glutamine (Thermo Fisher, Waltham, USA), 1× Pen-Strep (Thermo Fisher, Waltham, USA), 20 ng/ml of FGF-2 (Thermo Fisher, Waltham, USA), and 20 ng/ml EGF (Thermo Fisher, Waltham, USA)) to which 5.5 ml of Percoll/PBS solution was added. The tubes were mixed by inversion. Thereafter, another centrifugation step with 400g was performed for 15 min at RT. The cell pellet was washed three times with 10 ml NPC medium and spun down at 200g for 5 min at RT each time to collect the cells. Finally, the pellet was washed once more with 8 ml of NPC medium. The cell pellet was resuspended with 1 ml of DMEM-F12, and the cells were then plated onto 24-cm² cell culture plates. The cells were cultured in a 5% CO₂ incubator. The neurospheres were observed within 72 h. On day 3, growth factors (20 ng/ml of FGF-2 and 20 ng/ml EGF) were added to the cell culture. The cell passage period of NPCs was 5 to 6 days.

MSCs obtained from allogeneic adipose tissue of C57BL/J mice (25–30 g) were cultured. The adipose tissue was digested with collagenase (Sigma-Aldrich, St. Louis, USA). Primary MSCs were cultured in a T75 flask. Each flask contained 3.6×10^6 cells incubated under standard cell culture condition (37 °C, 5% CO₂) in MSC culture medium (DMEM F-12 medium, fetal bovine serum (FBS, Thermo Fisher, Waltham, USA), and 1× Pen-Strep (Thermo Fisher, Waltham, USA)). The cell passage period of MSCs was 6 to 7 days.

EV Enrichment from Cultured NPCs and MSCs

After passage 3, NPCs were treated with Accutase (Sigma-Aldrich, St. Louis, USA) and transferred to T75 cell culture flasks with 30 ml NPC culture medium without growth factors. Each T75 contained 36×10^6 NPCs. A total of 12 of T75 cell culture flasks were used in each EV isolation, meaning EVs from 432×10^6 cells were isolated. NPC-conditioned medium (NPC-CM) was collected after 24 h of incubation under standard cell culture conditions. Large vesicles and debris were removed by filtration through 220-nm pore filters (TPP Techno Plastic Products AG, Trasadingen, Switzerland). The NPC-CM was kept frozen (−80 °C) until further processing. After the thawing of the NPC-CM, EVs were enriched using the polyethylene glycol (PEG) precipitation method, as previously described [19, 33]. In brief, PEG precipitation was performed at a final concentration of 10% PEG 6000 (50% wt/vol; Merck Group, Darmstadt, Germany) and 75 mM NaCl. After incubation for 12 h at 4 °C, the EVs were concentrated by centrifugation for 45 min at 4500 g. EV pellets were resuspended in saline to a total volume of 30 ml and precipitated by ultracentrifugation for 2 h at 110,000g (Optima XPN-80 Ultracentrifuge, Beckman Coulter, Brea, USA). The target speed was 30,000 U/min, and both the acceleration and the brake were set to maximum. EV pellets were resuspended and diluted in saline to a concentration of 500 µl containing EVs obtained from CM of 432×10^6 NPCs. Aliquots of 500 µl each were stored at −80 °C until usage. The MSC-EV isolation was done after the third MSC passage. MSCs were cultured overnight with an FBS-free culture medium, and after 24 h, the cell supernatants were collected. EVs were obtained from these supernatants by using the same protocol as for the NPC-EV PEG isolation method.

Since the optimal enrichment procedure for NPC-EVs is still a matter for debate [19], we applied differential centrifugation, i.e., ultracentrifugation only, for some experiments. As such, some NPC-EV samples were treated with ultracentrifugation as described before without the application of PEG 6000. In brief, the cell culture medium was filtered through 220-nm filters to remove cell debris and apoptotic bodies followed by a 2-h ultracentrifugation procedure at 110,000g.

Nanoparticle Tracking Analyses

For both size determination and quantification of enriched NPC-EVs, a nanoparticle tracking analysis (NTA) was performed using the Nanosight platform (NanoSight LM10, Malvern Panalytical, Kassel, Germany). As shown previously [34], 1:1000 water-diluted samples were measured in duplicate, and 400 µl of the diluted sample was injected into the measurement chamber. Each sample was measured three times, and the length of the video of each measurement was set to 30 s.

Western Blot Analysis

Protein concentrations of EV samples were determined using the micro-bicinchoninic acid assay (Thermo Fisher, Waltham, USA). Western blots were performed with 5 µg of the concentrated EV fractions, which were treated with sample buffer (dithiothreitol, 0.1% SDS, 0.1 M Tris HCl; pH 7.0) and boiled for 5 min at 95 °C before separation on 12% SDS-polyacrylamide gel electrophoresis gels. The samples were transferred to polyvinylidene fluoride membranes (Merck Group, Darmstadt, Germany). The membranes were blocked by 5% milk solution (skim milk powder (Thermo Fisher, Waltham, USA) dissolved in Tris-buffered saline solution with 1% Tween-20) for 1 h at RT and stained with antibodies recognizing “exosomal marker” proteins including CD63 (1:500, Biorbyt, Cambridge, UK), TSG101 (1:500, GeneTex, Irvine, USA), Alix (1:500, BD Transduction Laboratories, San Jose, USA), and negative control calnexin (1:500, Abcam, Cambridge, UK) followed by a 1-h incubation with a matched horseradish peroxidase-labeled secondary antibody. Immunoreactivity was detected using chemiluminescence detection kit reagents and a Chemidoc Station (Biorad, Hercules, USA). ImageJ was used for densitometric analysis of each blot. The Western blotting procedures were repeated three times per sample. Please also refer to Supplementary Figure S2 for uncropped Western blots.

Transmission Electron Microscopy

Transmission electron microscopy (TEM) was used to investigate the microstructure of NPC-EVs. Briefly, formvar-coated TEM grids (copper, 150 hexagonal mesh, Science Services, Munich, Germany) were put on the top of a droplet of the respective EV fraction and incubated for 10 min. Then, the grids were washed five times by incubation for 2 min in PBS, followed by similar incubations with ultrapure water. For contrast, the grids were incubated for 5 min on droplets of uranylacetate-oxalate, followed by a 5-min incubation on droplets of a 1:9 dilution of 4% uranylacetate in 2% methylcellulose. These solutions were prepared as described as

before [35]. After draining the methylcellulose from the grids using a filter paper and drying of the methylcellulose film as previously described, samples were imaged with a LEO912 transmission electron microscope (Carl Zeiss Microscopy, Oberkochen, Germany) and images were taken using an on-axis 2k CCD camera (TRS-STAR, Stutensee, Germany).

Mass Spectrometric Analyses

NPC-EV samples were reconstituted in 1× NuPAGE LDS Sample Buffer (Invitrogen, Carlsbad, USA) and separated on 4–12% NuPAGE Novex Bis-Tris Minigels (Invitrogen, Carlsbad, USA). Gels were stained with Coomassie blue for visualization purposes, and each lane was sliced into 12 equidistant lanes regardless of staining. After washing, gel slices were reduced with dithiothreitol (DTT), alkylated with 2-iodoacetamide, and digested with trypsin overnight. The resulting peptide mixtures were then extracted, dried in a SpeedVac, reconstituted in 2% acetonitrile/0.1% formic acid (v:v), and prepared for nanoLC-MS/MS as described previously [36].

For the mass spectrometric analysis, samples were enriched on a self-packed reversed phase-C18 precolumn (0.15 mm ID × 20 mm, Reprosil-Pur120 C18-AQ 5 μm, Dr. Maisch, Ammerbuch-Entringen, Germany) and separated on an analytical reversed phase-C18 column (0.075 mm ID × 200 mm, Reprosil-Pur 120 C18-AQ, 3 μm, Dr. Maisch, Ammerbuch-Entringen, Germany) using a 30-min linear gradient of 5–35% acetonitrile/0.1% formic acid (v:v) at 300 nl min⁻¹. The eluent was analyzed on a Q Exactive hybrid quadrupole/orbitrap mass spectrometer (Thermo Fisher Scientific, Dreieich, Germany) equipped with a FlexIon nanoSpray source and operated under Excalibur 2.4 software using a data-dependent acquisition method. Each experimental cycle was of the following form: one full MS scan across the 350–1600-m/z range was acquired at a resolution setting of 70,000 FWHM, and the AGC target of 1 × 10⁶ and a maximum fill time of 60 ms. Up to the 12 most abundant peptide precursors of charge states 2 to 5 above a 2 × 10⁴ intensity threshold were then sequentially isolated at 2.0 FWHM isolation width, fragmented with nitrogen at a normalized collision energy setting of 25%, and the resulting production spectra recorded at a resolution setting of 17,500 FWHM, and AGC target of 2 × 10⁵ and a maximum fill time of 60 ms. Selected precursor m/z values were then excluded for the following 15 s. Two technical replicates per sample were acquired. Peak lists were extracted from the raw data using Raw2MSMS software v1.17 (Max Planck Institute for Biochemistry, Martinsried, Germany). Protein identification was achieved using MASCOT 2.5.1 software (Matrixscience, London, UK). Proteins were identified against the UniProtKB mouse reference proteome v2017.09 (16,930 protein entries) along with a set of 51 contaminants commonly identified in our laboratory.

The search was performed with trypsin as enzyme and iodoacetamide as a cysteine blocking agent. Up to two missed tryptic cleavages and methionine oxidation as a variable modification were allowed for. Search tolerances were set to 10 ppm for the precursor mass, 0.05 Da for fragment masses, and ESI-QUAD-TOF specified as the instrument type. For further information about the mass spectrometric analyses, please refer to [Supplementary Material](#) “mass spectrometric analyses” attachment.

NPC-EV RNA Isolation and qRT-PCR

In order to investigate whether or not NPC-EVs contain distinct sets of miRNAs that might be responsible for the biological effects of EVs on neuroprotection or neuroregeneration, we chose several miRNA candidates according to the literature [37–41]. Total RNA, including miRNAs, was extracted using TRIzol (Invitrogen, Carlsbad, USA) according to the manufacturer’s instructions. ANanoDropND1000 spectrophotometer (NanoDrop, Wilmington, DE, USA) was used to measure the RNA concentrations. The KAPA SYBR® FAST One-Step Kit for LightCycler®480 (Merck Group, Darmstadt, Germany) was used to perform qRT-PCR according to the manufacturer’s instruction request. The PCR primers were purchased from Eurofins Genomics and U6 as an internal control. miR-124: forward 5′-GCGA GGATCTGTGAATGCCAAA-3′ and reverse 5′-AGAT GGTGATGGGCTTCCC-3′, miR-145: forward 5′-GUCCAGUUUUCCAGGAAUCCCU-3′ and reverse 5′-GGAUUCCUGGGAAAACUGGACUU-3′, miR-17: forward 5′-GAGCCAAAGTGCTTACAGTGC-3′ and reverse 5′-AGTGCAGGGTCCGAGGTATT-3′, miR-19b: forward 5′-GGGCAAATCCATGCAAAAAC-3′ and reverse 5′-AGTG CAGGGTCCGAGGTATT-3′, miR-20a: forward 5′-TGGG TAAAGTGCTTATAGTGC-3′ and reverse 5′-AGTG CAGGGTCCGAGGTATT-3′, miR-26a: forward 5′-CCGC CGTTCAAGTAATCCAG-3′ and reverse 5′-AGTG CAGGGTCCGAGGTATT-3′, miR-26b: forward 5′-CGCC GCTTCAAGTAATTCAGGAT-3′ and reverse 5′-GTGC AGGGTCCGAGGT-3′, miR-23a: forward 5′-CAGG CGGGTAGTAGATG-3′ and reverse 5′-AGGG ACGGGCATGGAAAGG-3′, miR-126: forward 5′-CGCG CCGTACCGTGAGTAA-3′ and reverse 5′-GTGC AGGGTCCGAGGT-3′, U6: forward 5′-TCGC TTCGGCAGCACATA-3′ and reverse 5′-GGGC CATGCTAATCTTCTCTG-3′. The PCR cycling included reverse transcription stage at 42 °C for 5 min and 95 °C for 3 min followed by amplification stage at 95 °C for 10 s and 58 °C for 20 s. At the melting curve stage, the temperature was set to 95 °C for 5 s followed by 65 °C for 1 min and set the acquisition mode to continuous, duration mode set to 5–10 acq/°C; the temperature was 97 °C at the end. The cooling

stage was set to 40 °C for 10 s. miRNA expression was quantified using the $2^{-\Delta Ct}$ method.

Cerebral Organoids and Oxygen-Glucose Deprivation Assay

Cerebral organoids were generated from in-house generated iPSCs (hiPS-G1) [42] embedded in a collagen hydrogel (Zafeiriou et al., in revision). Directed differentiation was performed by dual SMAD inhibition (SB/noggin) in the presence of retinoic acid and subsequently supported by FGF-2, TGF- β 1, and DAPT exposure. Cerebral organoids on culture day 30 were used for analyses. Before the induction of oxygen-glucose deprivation (OGD), cerebral organoids were cultured in standard cortex culture medium in 24-well plates for 7 days. Thereafter, cerebral organoids were washed with PBS twice before induction of the OGD, using a commercially available hypoxia chamber (Toepffer Laborsysteme GmbH, Göppingen, Germany). For the induction of OGD, the cerebral organoids were incubated in glucose-free BSSO solution under hypoxic conditions for 8–10 h. The OGD chamber setting was as follows: 37 °C, O₂ less than 0.5%, CO₂ 5%, and humidity 70%. The amount of NPC-EVs applied to organoids was calculated by the following process: the EVs from 432×10^6 NPCs were diluted in 500 μ l of PBS, each microlitre contained 8.64×10^5 cell equivalent EVs (8.64×10^5 cell equivalent/ μ l, 43.2 μ g/ μ l). Three different NPC-EV concentrations were tested: NPC-EVs low (EVs equivalent to 2×10^5 NPCs, i.e., 1 μ g of NPC-EVs), NPC-EVs medium (EVs equivalent to 2×10^6 NPCs, i.e., 10 μ g of NPC-EVs), NPC-EVs high (EVs equivalent to 2×10^7 NPCs, i.e., 100 μ g of NPC-EVs). EVs were carefully vortexed for 1 min before applying to organoids in order to prevent any aggregation of EVs. After hypoxia, the organoids were taken out from the hypoxia chamber followed by 24 h of reoxygenation with normal cell culture medium in an incubator (5% CO₂) under standard cell culture conditions. The EVs were added to the organoids at the beginning of the OGD and at the beginning of the reoxygenation. Terminal deoxynucleotidyl transferase dUTP nick end labeling (TUNEL, In Situ Cell Death Detection Kit, Merck Group, Darmstadt, Germany) staining was used according to the manufacturer guidance in order to detect cell death rates, and 4',6-diamidino-2-phenylindole (DAPI) staining was used in order to stain nuclei.

Experimental Paradigm and Animal Groups

No human samples were used for the study. All studies were performed with governmental approval according to the NIH guidelines for the care and use of laboratory animals. Both the STAIR criteria and the ARRIVE guidelines were followed. Male C57BL6 mice aged 10 weeks (Harlan Laboratories, Darmstadt, Germany) were kept

under circadian rhythm with free access to food and water. The mice were randomly assigned to the treatment groups. At all stages of the study, the researchers were blinded from the experimental conditions chosen. Middle cerebral artery occlusion (MCAO) was induced. Animals were anesthetized at 2 to 2.5% isoflurane during the MCAO surgery. A heating pad set to 37.0 °C was put under the animal to keep the body temperature at normal. The left common carotid artery (LCCA), left external carotid artery (LECA), and left internal carotid artery (LICA) were carefully dissected from the surrounding nerves and tissues. A permanent ligation was made on the LCCA and LECA, and a free knot was also made on the LICA. A silicon-coated monofilament (Doccol Corp., Sharon, USA) was inserted into the LCCA and then gently pushed forward toward the offspring of the left middle cerebral artery (MCA) through a small hole which was cut on the LCCA until a significant drop of the blood flow on the laser Doppler flow (LDF) recording was observed. During the experiment, the LDF was recorded with a flexible probe (Perimed AB, Järfälla, Sweden) above the core of the left MCA territory. A drop in the blood flow of more than 80% to the baseline was considered to indicate successful surgery. Sixty minutes after monofilament insertion, the reperfusion was initiated by monofilament removal, and the LDF recordings were continued for an additional 15 min before the wounds were carefully sutured. The amount of NPC-EVs applied to organoids was calculated by the following process. The EVs from 432×10^6 NPCs were diluted to 500 μ l with PBS, and each microliter contains 8.64×10^5 cell equivalent EVs (8.64×10^5 cell equivalent/ μ l, 43.2 μ g/ μ l). The mice were exposed to MCAO followed by administration of normal saline (control), NPC-EVs medium (EVs equivalent 2×10^6 NPCs, 10 μ g), NPC-EVs low (EVs equivalent 2×10^5 NPCs, 1 μ g), or NPC-EVs high (EVs equivalent 2×10^7 NPCs, 100 μ g), MSC-EVs medium (EVs equivalent 2×10^6 MSCs, 10 μ g), MSC-EVs low (EVs equivalent 2×10^5 MSCs, 1 μ g), or MSC-EVs high (EVs equivalent 2×10^7 MSCs, 100 μ g). The result of the power calculation was 0.8372017 for both behavioral test analysis and immunofluorescence analysis, assuming an effect size of 0.4399022. EVs were carefully vortexed for 1 min before injection in order to prevent aggregation of EVs. The latter was suspended in 100 μ l PBS before injection. The administration occurred 24 h after the stroke via right femoral vein injection. The procedure was repeated for all experimental groups (saline and EV groups) on day 3 and on day 5 post-stroke using retroorbital injection techniques in order to avoid bilateral femoral vein injections. All samples were injected at a rate of 250 μ l over 10 min. The mice were allowed to survive for a maximum of 84 days. These mice were used for the behavioral

analyses and the immunofluorescence staining studies of brain injury and neurorestoration. Precise numbers of animals used are given for each condition in the figure legends and in the Supplementary Table S1 including survival rates of mice.

In Vivo Biodistribution Study of NPC-EVs

Three animals per group were used for the evaluation of EV biodistribution after different administration methods and conditions (femoral vein injection in sham mice, femoral vein injection after MCAO, retroorbital injection in sham mice, and retroorbital injection after MCAO). The EVs were labeled with Celltracker CM-DiI (Invitrogen, Carlsbad, USA) according to the manufacturer's instruction. In brief, DiI was incubated with EVs (EV equivalent 2×10^6 NPCs, 10 μ g) at 37 °C for 1 h. In the MCAO group, labeled EVs were injected into mice after MCAO surgery. Mice were sacrificed 2 h after the injection. Cryosections (14 μ m thick) of the brain, the lung, and the liver were counterstained with 4',6-diamidino-2-phenylindole (DAPI), and the biodistribution was analyzed by immunofluorescence staining. Images were acquired using an Axioplan 2 imaging microscope (Carl Zeiss AG, Hombrechtikon, Germany). Mean fluorescence intensity was measured by the ImageJ (version 1.80).

Flow Cytometry

Single-cell suspensions were prepared for flow cytometry. The mice were exposed to MCAO followed by administration of normal saline (control), NPC-EVs low (EVs equivalent to 2×10^5 NPCs, 1 μ g), NPC-EVs medium (EVs equivalent to 2×10^6 NPCs, 10 μ g), or NPC-EVs high (EVs equivalent to 2×10^7 NPCs, 100 μ g) at days 1, 3, and 5 after surgery. The power calculation of the flow cytometry analysis yielded 0.8243373 with an assumed effect size of 0.8596798. The mice were sacrificed by an overdose of isoflurane at day 7 after surgery. Blood samples were collected into EDTA-coated tubes by puncture of the inferior vena cava followed by transcranial perfusion with ice-cold 0.1 M PBS and brain removal. Erythrocytes were lysed by incubation with lysis buffer (155 mM NH_4Cl , 10 mM KHCO_3 , 3 mM EDTA) for 5 min followed by two washing steps with 0.1 M PBS. The ischemic part of the brain was dissected, followed by centrifugation and separation using a Percoll-gradient. Leukocyte and inflammatory cells were isolated from the intermediate phase. Cell suspension from the brain and blood was blocked with Fc-block (CD16/32 FcX rat anti-mouse IgG, BioLegend, San Diego, USA) to interrupt non-specific binding and afterwards stained for CD45 (CD45 rat anti-mouse IgG-brilliant Violet 510, BD Horizon, Franklin Lakes, USA), CD3 (CD3 rat anti-mouse IgG- PE, BD Horizon, Franklin Lakes, USA), CD19 (CD19 rat anti-mouse IgG-APC, BD Horizon, Franklin

Lakes, USA), and CD11b (CD11b rat anti-mouse IgG-PE-Cy7, eBioscience, Darmstadt, Germany). For data analysis, FlowJo v10.0 software was used. Please also refer to Supplementary Table S2 and Supplementary Figure S1 for further information.

Analysis of Post-Stroke Motor Coordination Deficits

The mice were trained on days 1 and 2 before the induction of stroke to ensure proper test behavior. The tests for analysis of motor coordination were performed at the time points given using the tight rope test, the balance beam test, and the corner turn test, as previously described [43]. The tight rope test and the balance beam test were performed three times on each test day, and the mean values were calculated. For the balance beam test, the readout parameter was the time until the mice reached the platform, with a maximal testing time of 60 s. Assessment of the tight rope test results was done using a validated score ranging from 0 (minimum) to 20 (maximum). The corner turn test included 10 trials per test day, during which the laterality index (number of left turns/10) was calculated. The details of the tight rope test score sheet can be found in Supplementary Table S3.

Immunofluorescence Staining

Brain injury as indicated by neuronal density was evaluated in 16- μ m cryostat sections stained with a mouse monoclonal anti-NeuN antibody (1:500; Merck Group, Darmstadt), which was detected by a goat anti-mouse Alexa Fluor 488 antibody (Invitrogen, Carlsbad, USA). For analysis, the regions of interests (ROIs) were defined at anterior-posterior +0.14 mm, medial-lateral \pm 1.15 to 2.25 mm, and dorsal-ventral -2.25 to 3.25 mm. Five sections per mouse were analyzed, and in each section, five ROIs were examined. The mean neuronal densities were determined for all ROIs. Endogenous cell proliferation and differentiation of newborn cells were analyzed after a single daily i.p. injection of 5-bromo-2-deoxyuridine (BrdU; 50 mg/kg body weight; Sigma-Aldrich, St. Louis, USA) from days 40 to 84. The sections were counterstained for BrdU and doublecortin (Dcx; immature neuronal marker) and NeuN (mature neuronal marker). A monoclonal mouse anti-BrdU (1:400; Roche Diagnostics, Basel, Switzerland), a monoclonal rat anti-BrdU (1:400; Abcam, Cambridge, UK), a polyclonal goat anti-Dcx (1:50; Santa Cruz Biotechnology, Heidelberg, Germany), and a monoclonal mouse anti-NeuN (1:350; Merck Group, Darmstadt, Germany) were used. All primary antibodies were detected using appropriate Cy-3-labeled or Alexa Fluor 488-labeled secondary antibodies (Jackson Immuno, West Grove, USA) followed by DAPI staining.

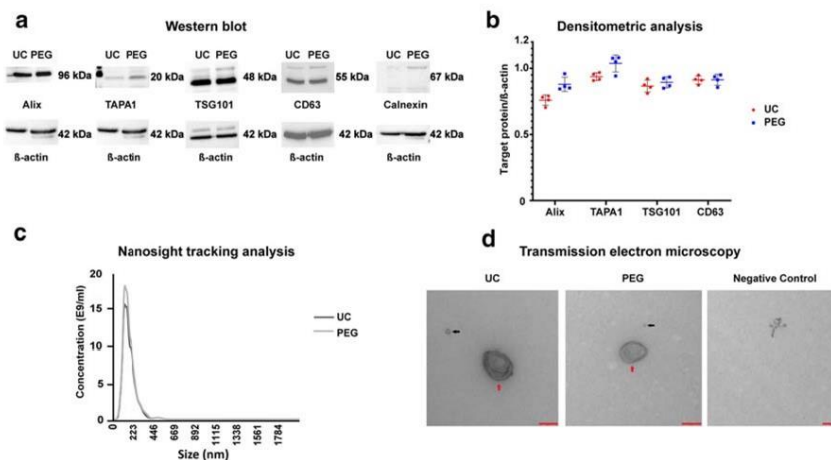


Fig. 1 Western blotting, nanosight tracking analysis (NTA), and transmission electron microscopy (TEM) of enriched NPC-EVs. Neural progenitor cells (NPCs) were cultured under standard cell culture conditions, and conditioned medium was obtained at passage 3 at 24 h after cell seeding. Conditioned medium was used for the enrichment of extracellular vesicles (EVs) using either the polyethylene glycol (PEG) method or differential centrifugation (i.e., ultracentrifugation). **a** Western blot analysis of EVs ($n = 4$ per isolation conditions) against exosomal markers, with calnexin being used as a negative marker and β -actin serving as a

loading control. **b** Densitometric analysis from Western blot analysis from **a**. **c** NTA from enriched EVs depicting size distribution patterns. **d** Representative TEM analysis from EVs enriched by either differential centrifugation (UC) or the PEG method. The negative control consisted of PBS only, depicting an artifact with no vesicular structure. Black arrows: exosomes; red arrows: microvesicles. Scale bar, 200 nm. EV, extracellular vesicles; PBS, phosphate-buffered saline; PEG, polyethylene glycol; NPC, neural progenitor cell; NTA, nanosight tracking analysis; TEM, transmission electron microscopy; UC, ultracentrifugation

For axonal plasticity, the anterograde tract tracer biotinylated dextran amine (BDA) was applied by stereotactic injection into the contralateral non-impaired cortex on day 70 post-stroke. As such, mice were deeply anesthetized and fixed into a stereotactic frame (ASI instruments, SAS-4100, Warren, USA). BDA was injected using a Hamilton syringe at 0.5 mm rostral from bregma, 2.5 mm lateral from the midline, and 1.5 mm ventral from the cortical surface. The syringe was kept in place for an additional 5 min after the end of the injection. A BDA detection kit (Life Technologies, Carlsbad, USA) was used after the sacrifice of the animals following the manufacturer's instructions.

Statistical Analysis

For comparison of two groups, the two-tailed independent Student t test was used. For comparison of three or more groups, a one-way analysis of variance (ANOVA) followed by the Tukey post hoc test and, if appropriate, a two-way ANOVA was used. G*Power was used to calculate the power of the experiment and GraphPad Prism was used for statistics. Unless otherwise stated, data are presented as mean with SD values. A p value < 0.05 was considered statistically significant.

Results

Characterization of NPC-EVs

Since the optimal procedure for EV enrichment remains uncertain [19], we systematically analyzed NPC-EVs using both the PEG method and ultracentrifugation only. The subsequent characterization of such enriched NPC-EVs included the transmission electron microscopy (TEM), nanosight tracking analysis (NTA), mass spectrometry, and Western blotting. Western blot analysis for selected EV biomarkers revealed that CD63, TSG101, TAPA1, and Alix were present in NPC-EVs obtained from both PEG enrichment and ultracentrifugation only (Fig. 1a, b). No difference was observed with regard to quantitative analysis of these proteins.

NTA revealed the distribution of NPC-EVs to be in the range of 30 to 300 nm, which is typical of exosomes and microvesicles alike (Fig. 1c). The concentration between the two isolation methods was similar (18×10^9 in the PEG method compared with 15×10^9 in the ultracentrifugation only method). Along with the NTA, experiments using TEM revealed a typical EV morphology (Fig. 1d). Furthermore, no other types of vesicles were found in our samples, suggesting that NPC-EVs were predominantly exosomes and microvesicles.

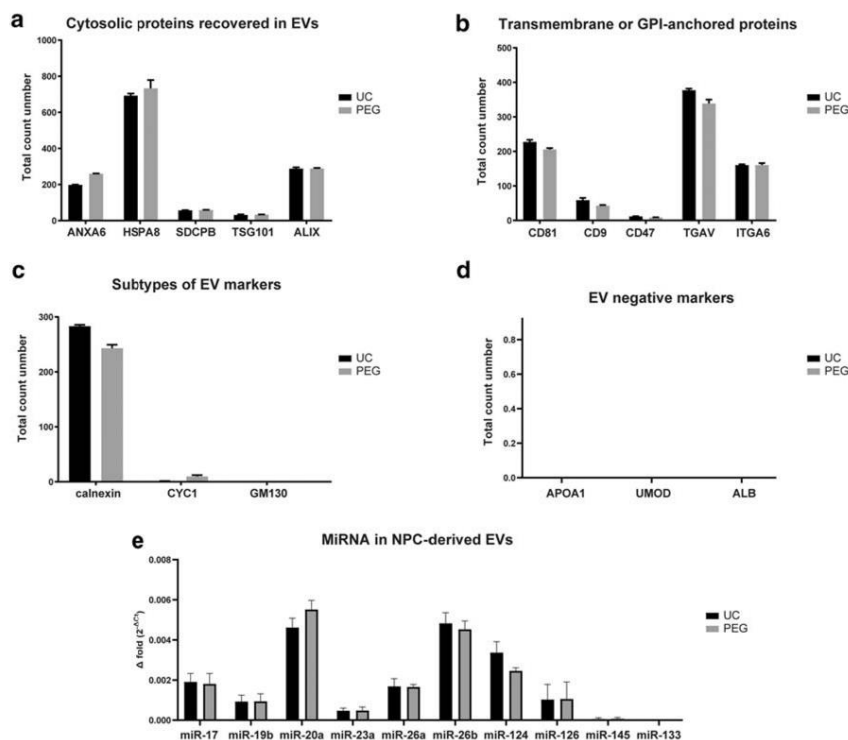


Fig. 2 Mass spectrometric analysis and qRT-PCR analysis of selected proteins and miRNAs in NPC-derived EVs. NPC-EVs were enriched using the PEG approach or ultracentrifugation as described before. Summed spectral counts of selected proteins from triplicate measurements are displayed. **a** Detection of cytosolic proteins including exosomal markers such as HSPA8, TSG101, and Alix. **b** Detection of transmembrane or GPI-anchored proteins in the two EV fractions. **c** Detection of intracellular proteins. Calnexin was found in both NPC-EV samples, although it is usually regarded as a negative control. Recent data,

however, suggests that calnexin can also be found in several exosomal subtypes (see the appropriate results section). **d** Detection of exosomal negative markers APOA1, UMOD, and ALB. These markers were detected neither PEG-enriched nor in ultracentrifugation-enriched EVs. **e** Screening for selected miRNAs using qRT-PCR in NPC-EVs enriched with the PEG method or with ultracentrifugation only. The results are presented as $2^{-\Delta\Delta Ct}$. EV, extracellular vesicles; NPC, neural progenitor cell; PBS, phosphate-buffered saline; PEG, polyethylene glycol method; UC, ultracentrifugation only method

By using mass spectrometric analyses, we successfully detected proteins which are crucial for EV biogenesis or are known to be associated with stimulated angiogenesis and neurogenesis such as HSP70, both in PEG-enriched and in ultracentrifugation-enriched NPC-EVs (please also refer to the [supplementary](#) section). EV cytosolic proteins, transmembrane proteins, or GPI-anchored proteins, which are crucial for EV biogenesis, such as ANXA6, SDCPB, HSPA8, TSG101, CD81, and CD9, were found in the EV samples (Fig. 2a, b). There was no significant difference between the two groups with respect to cytosolic or transmembrane proteins. Although calnexin was considered a negative control for EVs, calnexin can also be found in some subtypes of exosomes [19]. Other subtypes of exosomal markers such as

GM130 and CYC1 were close to the detection threshold or not detectable at all (Fig. 2c). Furthermore, strict EV negative markers (as purity control) such as APOA1, UMOD, and ALB were close to the detection threshold or not detectable at all in PEG or the ultracentrifugation group (Fig. 2d), suggesting a sufficiently high level of purification in EVs enriched with either PEG or ultracentrifugation.

Since miRNAs support angiogenesis, neurogenesis, and neuroprotection [44], we chose some of those miRNA candidates which have been identified as beneficial in the aforesaid aspects. Indeed, typical miRNA candidates were found in NPC-derived EVs, with the subtypes miR-20a, miR-26b, and miR-124 being at the highest concentrations (Fig. 2e). Conversely, miR-133 and miR-145 were hardly found in

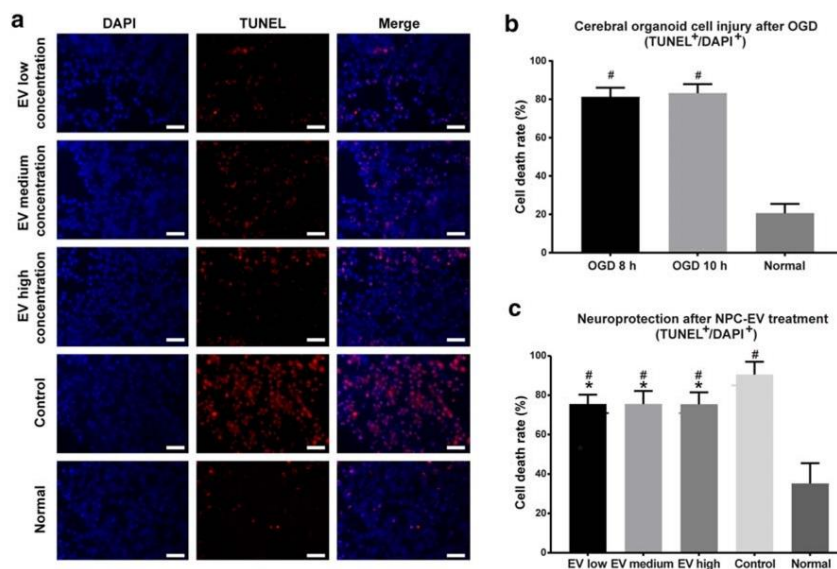


Fig. 3 NPC-EVs enhance the resistance of cerebral organoids exposed to oxygen-glucose deprivation (OGD). Cerebral organoids were obtained and cultured under standard cell culture conditions, as explained in the “Materials and Methods” section. **a** Representative photos from EV-treated cerebral organoids, as described in c. **b** The temporal resolution of the development of cell death under OGD conditions was determined for cerebral organoids ($n = 3$ per condition) exposed to 8 h or 10 h of OGD, followed by reoxygenation under standard cell culture conditions for an additional 24 h. Cell death rates were assessed using TUNEL staining on cryostat sections, with DAPI staining for nuclear detection. **c** Since no statistical significance of cell death rates of organoids exposed to either 8 h or 10 h of OGD was observed, further experiments were done using the 8-h time window only. Organoids were treated with NPC-derived EVs at the beginning of the OGD and additionally at the beginning of the reoxygenation. Three different NPC-EV concentrations were

chosen ($n = 3$ per condition), i.e., NPC-EVs low (EVs equivalent to 2×10^5 NPCs), NPC-EVs medium (EVs equivalent to 2×10^6 NPCs), and NPC-EVs high (EVs equivalent to 2×10^7 NPCs). Control organoids were exposed to OGD only without EV treatment, whereas “normal” refers to cerebral organoids kept under standard cell culture conditions. Scale bars, 20 μ m. Asterisk indicates significant difference from controls with $p < 0.05$, i.e., NPC-EVs low, $p = 0.0015$; NPC-EVs medium, $p = 0.0015$; and NPC-EVs high, $p = 0.0014$. Number sign indicates significant difference from standard cell culture conditions (normal) with $p < 0.05$, i.e., OGD 8 h or OGD 10 h, $p < 0.0001$; NPC-EVs low, $p < 0.0001$; NPC-EVs medium, $p < 0.0001$; NPC-EVs high, $p < 0.0001$. EV, extracellular vesicles; OGD, oxygen-glucose deprivation; PBS, phosphate-buffered saline; NPC, neural progenitor cell; TUNEL, terminal deoxynucleotidyl transferase dUTP nick end labeling

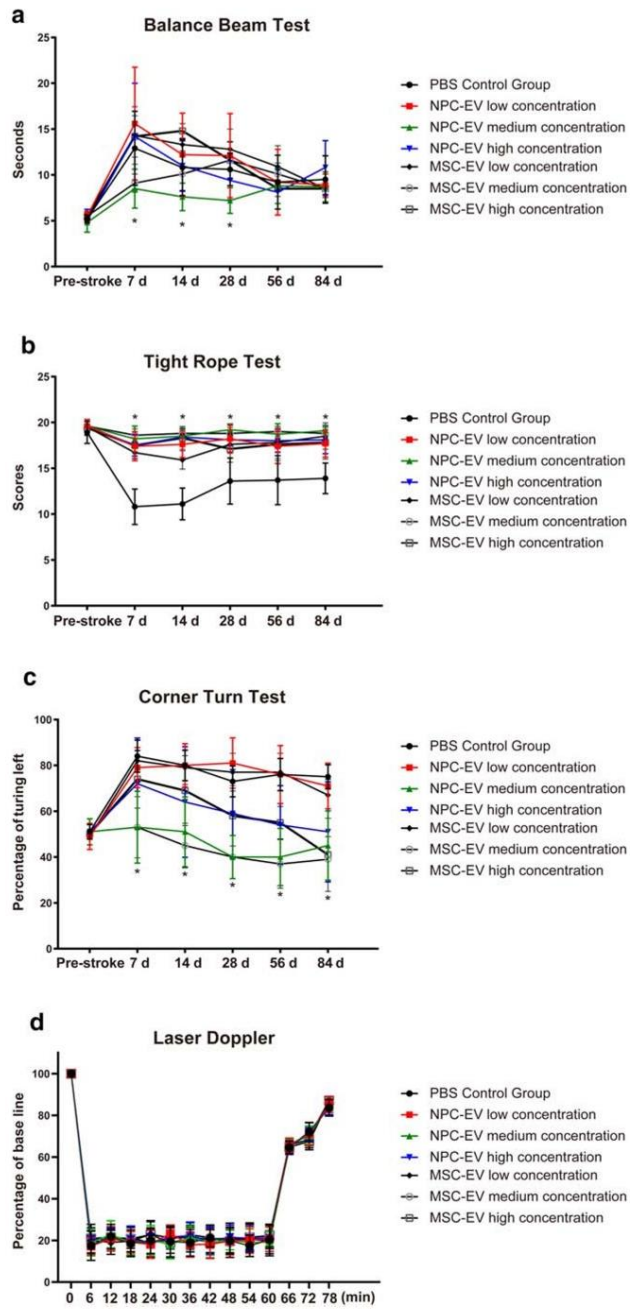
NPC-derived EVs at all. The isolation method, however, did not significantly affect these miRNA levels in NPC-EVs.

Since both enrichment procedures did not significantly differ between each other for the majority of the readout parameters analyzed for NPC-EV characterization, further experiments were performed using the PEG method only. In this context, the PEG approach is more feasible than ultracentrifugation, allowing the handling of large volumes of conditioned medium with ease.

NPC-EVs Protect Cerebral Organoids from Oxygen-Glucose Deprivation

After having characterized the aforementioned EVs, we then established an in vitro model of the OGD in cerebral organoids, which better reflect the physiological situation than

neuronal monolayer cultures do. We first tested the time course of OGD-induced cell death of cerebral organoids by exposing the organoids to either 8 h or 10 h of OGD, followed by 24 h of reoxygenation under standard cell culture conditions (Fig. 3a, b). Cell death rates under these conditions were significantly increased in organoids exposed to both 8 h and 10 h of OGD when compared with cerebral organoids that were kept under standard culture conditions (Fig. 3b). However, no significant difference was found between the two OGD groups themselves. Accordingly, we chose an OGD exposure of 8 h for the following experiments. Cerebral organoids were then treated with low, medium, or high concentrations of NPC-derived EVs, and the cell death rate was measured after 8 h of OGD followed by 24 h of reoxygenation (Fig. 3c). Indeed, exposure to all three concentrations of NPC-EVs significantly reduced the cell death rate



◀ **Fig. 4** Delivery of NPC-EVs reduces post-ischemic motor coordination impairment. Motor coordination was evaluated using the balance beam test (a), the tight rope test (b), and the corner turn test (c) at 1, 7, 14, 28, 56, and 84 days after cerebral ischemia. All animals were accordingly trained before the induction of stroke in order to ensure proper test performance, i.e., test results before induction of stroke are given as pre-stroke data. Mice were exposed to 1 h of middle cerebral artery occlusion with subsequent reperfusion. Mice received systemic delivery of PBS (control, $n = 11$), NPC-EVs low (EVs equivalent to 2×10^5 NPCs, $n = 12$), NPC-EVs medium (EVs equivalent to 2×10^6 NPCs, $n = 11$), or NPC-EVs high (EVs equivalent to 2×10^7 NPCs, $n = 12$), MSC-EVs low (EVs equivalent to 2×10^5 MSCs, $n = 12$), MSC-EVs medium (EVs equivalent to 2×10^6 MSCs, $n = 12$), or MSC-EVs high (EVs equivalent to 2×10^7 MSCs, $n = 13$) 24 h, 72 h, and 120 h post-stroke. The first injections at 24 h were done via cannulation of the right femoral vein, whereas the following injections used a retroorbital injection delivery. All EV dosage groups showed significant improvement in the tight rope test compared with the control group ($p < 0.0001$). In the corner turn test, the EV medium concentration group showed improvement at all experimental time points ($p < 0.0001$ in NPC-EV medium group, $p < 0.0001$ in MSC-EV medium group), and the EV high dosage group showed improvement at day 56 ($p = 0.0002$ in NPC-EV high group, $p = 0.0004$ in MSC-EV high group) and at day 84 ($p < 0.0001$ in NPC-EV high group, $p < 0.0001$ in MSC-EV high group) compared with the control group. In the balance beam test, however, only the EV medium group showed improvement at day 7 ($p = 0.0006$ in NPC-EV medium group, $p = 0.0040$ in MSC-EV medium group), day 14 ($p = 0.023$ in NPC-EV medium group, $p = 0.0021$ in MSC-EV medium group), and day 28 ($p = 0.0129$ in NPC-EV medium group) compared with the control group. **d** Laser Doppler results of different experimental groups during MCAO operation. Asterisk indicates significant difference from controls with $p < 0.05$. PBS, phosphate-buffered saline; MSC, mesenchymal stem cells; NPC, neural progenitor cell; EV, extracellular vesicles

of cerebral organoids under these conditions, as assessed by the TUNEL staining.

Delivery of NPC-EVs Reduces Post-Ischemic Motor Coordination Impairment

In light of the aforementioned in vitro data on cerebral organoids, we tested the hypothesis that NPC-EVs improve neurological recovery after cerebral ischemia in mice. Following a previously published protocol on MSC-EVs [17], NPC-EVs of different dosages (low, medium, and high) were systemically administered on days 1, 3, and 5 post-stroke, with MSC-EVs serving as internal controls (Fig. 4a–c). Administration of a medium dosage of both NPC-EVs and MSC-EVs resulted in significantly better test performance of these animals in the tight rope test as well as in the corner turn test when compared with controls (Fig. 4b, c). Of note, NPC-EVs were not inferior to MSC-EVs, and the better test performance of mice treated with either NPC-EVs or MSC-EVs was long lasting and thus stable until the end of the observation period of 84 days. In the balance beam test, however, the beneficial effects of NPC-EVs and MSC-EVs delivered at a medium dose were only transiently effective (Fig. 4a). Delivery of NPC-EVs or MSC-EVs at low or high dosages only partially induced

neurological recovery in these three tests, if at all. The laser Doppler flow was used to ensure the quality of the MCAO model in each group. Each group showed a significant blood flow drop during the surgery, and there was no significant difference between the various treatment groups (Fig. 4d).

Neurological recovery does not necessarily imply an effect on brain tissue injury or brain regeneration and vice versa. We subsequently analyzed neuronal survival in the ischemic striatum at 84 days after the stroke. In line with the reduction of neurological impairment, increased neuronal densities were found in mice treated with medium doses of both NPC-EVs or MSC-EVs (Fig. 5a), again showing no difference between these two groups. Low and high doses of NPC-EVs or MSC-EVs were not effective. Conclusively, NPC-derived EVs reduce post-stroke brain injury on both the histological and the functional levels and are not inferior to MSC-derived EVs. It is important to note that the therapeutic effect in EV formulation was highly dose-dependent.

NPC-EV Delivery Stimulates Post-Stroke Neuroregeneration and Axonal Plasticity

As stated before, neurological recovery is not always associated with histological changes, and the mechanisms that lead to enhanced neurological recovery are diverse. In this context, we hypothesized that NPC delivery might stimulate endogenous repair mechanisms of the brain, including increased levels of neurogenesis. Taking into account that neurogenesis also takes place in the adult mammalian brain, with endogenous stem cells being stimulated upon induction of cerebral ischemia, the application of NPC-EVs might positively interfere with this process. Indeed, analysis of the cell proliferation marker BrdU showed significantly increased levels of BrdU⁺ cells (Fig. 5b) in the NPC-EV medium group. The co-expression analysis with the proliferation marker BrdU and the neuronal marker NeuN revealed increased levels of NeuN⁺/BrdU⁺ cells on day 84 within the ischemic striatum of animals treated with a medium dosage of NPC-EVs (Fig. 5c). On the contrary, the relative amount of BrdU⁺ cells expressing the immature neuronal marker Dcx was not affected by NPC-EV-treatment (Fig. 5d).

Neuroregeneration is a complex process that is not only limited to neurogenesis. We therefore investigated the extent of axonal plasticity on day 84 in the post-ischemic brain (Fig. 6), using contralateral stereotactic injections of BDA in the non-impaired cortex. Again, delivery of a medium dose of NPC-EVs but not low or high doses of NPC-EVs significantly enhanced axonal plasticity in these mice when compared with the control group (Fig. 6). Treatment with a medium dosage of MSC-EVs yielded similar effects with regard to neuroregeneration and axonal plasticity as observed for NPC-EVs, suggesting again that NPC-EVs are not inferior to MSC-EVs.

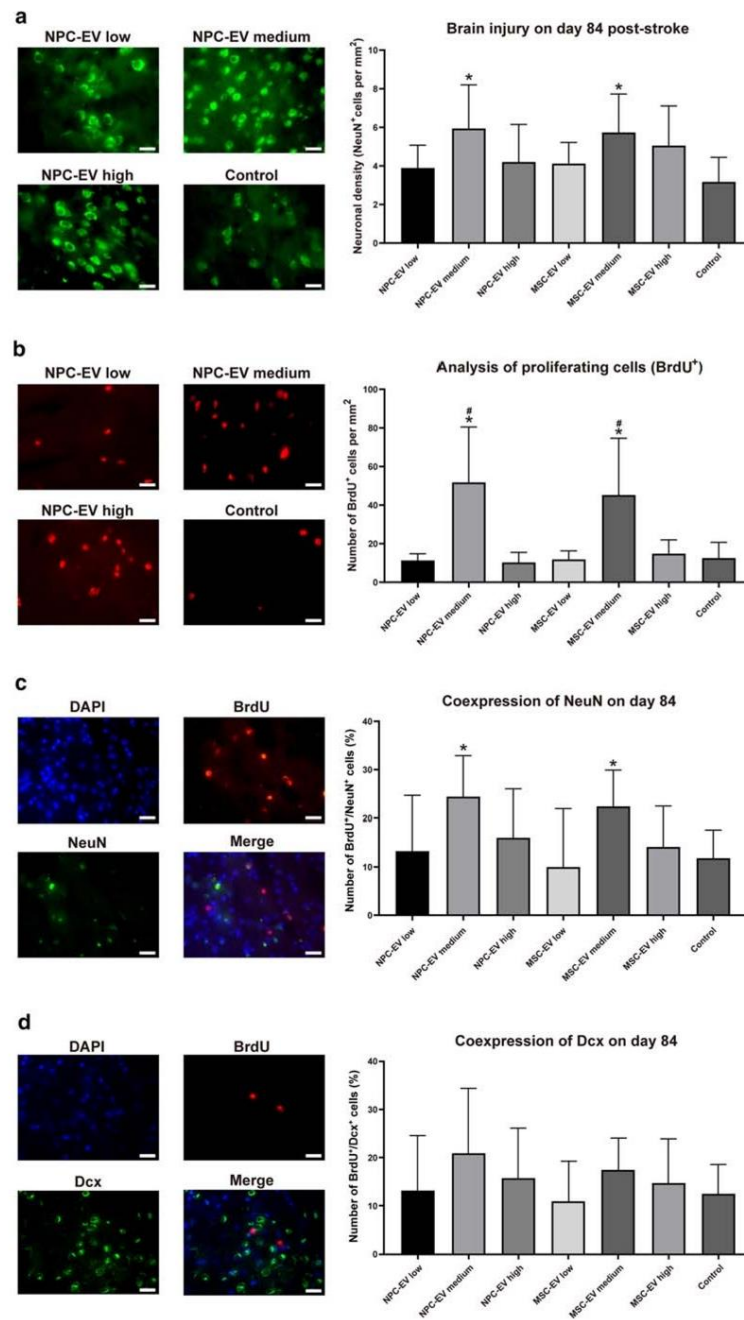


Fig. 5 NPC-EVs induce long-term neuroprotection and increase cell proliferation after stroke. The neuronal density **a** and cell proliferation **b** were measured on day 84, as indicated by NeuN staining (**a**) within the ischemic lesion site and cell proliferation, as indicated by BrdU staining (**b**) in order to investigate. The extent of neurogenesis was analyzed on day 84, as indicated by the neuronal marker NeuN (**c**) and the immature neuronal marker Dcx (**d**). Co-immunofluorescence staining was done with the cell proliferation marker BrdU. Mice were exposed to 60 min of focal cerebral ischemia and treated with EVs at different dosages. The first injections at 24 h were done via cannulation of the right femoral vein, whereas the following injections used a retroorbital injection delivery. Mice were exposed to middle cerebral artery occlusion followed by systemic delivery of PBS (control, $n = 11$), NPC-EVs low (EVs equivalent to 2×10^5 NPCs, $n = 12$), NPC-EVs medium (EVs equivalent to 2×10^6 NPCs, $n = 11$), or NPC-EVs high (EVs equivalent to 2×10^7 NPCs, $n = 12$), MSC-EVs low (EVs equivalent to 2×10^5 MSCs, $n = 12$), MSC-EVs medium (EVs equivalent to 2×10^6 MSCs, $n = 12$), or MSC-EVs high (EVs equivalent to 2×10^7 MSCs, $n = 13$) 24 h, 72 h, and 120 h post-stroke. Photos depict representative stainings from the respective condition. Both NPC-EV medium and MSC-EV medium groups increased neuronal density, as shown in (**a**; $p = 0.0007$ in NPC-EV medium group, $p = 0.0022$ in MSC-EV medium group) and stimulated endogenous cell proliferation (**b**; $p < 0.0001$ in NPC-EV medium group, $p < 0.0001$ in MSC-EV medium group). Newborn neurons were also increased in NPC-EV medium and MSC-EV medium groups (**c**; $p = 0.0015$ in NPC-EV medium group, $p = 0.0037$ in MSC-EV medium group). The NPC-EV medium and MSC-EV medium group also showed higher cell proliferation levels compared with NPC-EV or MSC-EV high or low dosage groups (**b**; $p < 0.0001$ in NPC-EV medium group, $p < 0.0001$ in MSC-EV medium group compared with the low or high dosage NPC-EV or MSC-EV groups). However, there was no significant difference between the NPC-EV medium group and the MSC-EV medium group. Scale bars, 20 μm . Asterisk indicates significant difference from controls with $p < 0.05$. Number sign indicates significant difference from low or high dosage NPC-EV or MSC-EV groups with $p < 0.05$.: BrdU, 5-bromo-2-deoxyuridine; DAPI, 4',6-diamidino-2-phenylindole; Dcx, doublecortin; EV, extracellular vesicles; MSC, mesenchymal stem cells; NPC, neural progenitor cell; PBS, phosphate-buffered saline

NPC-EVs Reverse Peripheral Post-Stroke Immunosuppression

The pathophysiology of cerebral ischemia comprises of a complex string of diverse inflammatory signaling cascades, not solely being harmful to the surrounding ischemic tissue [45]. In our previous study, MSC-EVs did not affect the immune response in the central nervous system but reversed the post-ischemic immunosuppression in the peripheral blood 7 days after stroke. In NPC-EVs, we saw similar effects. Consequently, NPC-EV treatment of mice with either dosage did not affect leukocytes ($\text{CD45}^{\text{high}}$), monocytes ($\text{CD45}^{\text{high}}\text{CD3}^-\text{CD11b}^+$), B cells ($\text{CD45}^{\text{high}}\text{CD3}^-\text{CD19}^+$), or T cells ($\text{CD45}^{\text{high}}\text{CD3}^+$) within the ischemic CNS (Fig. 7a–d). The flow cytometry analysis of the blood of mice treated with a medium but not a low or high dosage of NPC-EVs revealed significantly increased levels of both B lymphocytes and T lymphocytes when compared with that the control group (Fig. 7e–h).

NPC-EVs Predominantly Distribute in Peripheral Organs

The majority of MSCs and other transplanted cells do not reach the brain, but are trapped in extracranial organs [46]. Even though EVs are known to pass the blood-brain barrier [47], the fact that NPC-EVs predominantly modulated the peripheral but not the central immune system (Fig. 8) might suggest that the majority of EVs do not reach the brain, either. Since different administration methods and conditions might affect the biodistribution patterns of NPC-EVs, we compared two different delivery routes, i.e., femoral vein injection and retroorbital injection under both ischemic and non-ischemic conditions. The biodistribution of NPC-EVs was similar in different methods and different conditions (Fig. 8). NPC-EVs were not only found in peripheral organs such as the liver and the lung but also found in the brain. However, most of these EVs were detected in the liver and in the lung when compared with the brain. There was no difference between the liver and the lung with regard to NPC-EV biodistribution patterns.

Discussion

Although EVs have recently been recognized as potential therapeutic tools in the treatment of stroke [48], previous work has almost exclusively focused on the application of MSC-derived EVs only [17]. As such, the relevance of the stem cell source for EV enrichment remains elusive, although recent data on pluripotent stem cell-derived NSC-EVs has become available [49, 50]. The present study elucidated whether or not EVs have a cell-type independent therapeutic potential against stroke that is not restricted to MSC-derived EVs. The latter will be of high therapeutic relevance under clinical stroke conditions in order to choose proper tissue sources or pooled fractions from cell sources beyond MSCs or related cells. Since both endogenous and grafted SVZ-derived NPCs contribute to neurological recovery and neuroregeneration upon experimental stroke [51], EVs from such SVZ-derived NPCs have been enriched in the present study. We provide evidence for NPC-EVs not only for increasing cell resistance against hypoxic injury in vitro but also for enhancing post-stroke neuroregeneration and neurological recovery in vivo. Applying a direct comparison against MSC-EVs, for the first time, we demonstrate that SVZ-derived NPC-EVs exhibit a similar therapeutic activity as MSC-EVs in a mouse model of stroke.

In light of various EV enrichment procedures, i.e., ultracentrifugation, precipitation, chromatography, or density gradient separation [52], the optimal enrichment technique is still a matter of debate [19]. The pros and cons of each technique have to be thoroughly balanced when being applied. In that

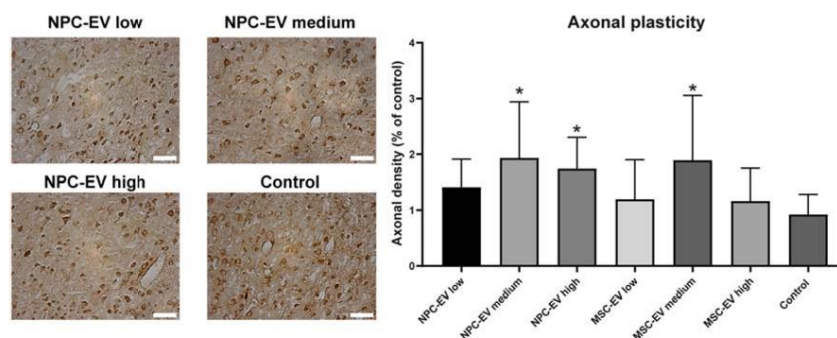


Fig. 6 NPC-EV delivery affects post-ischemic axonal plasticity. Mice were exposed to 60 min of focal cerebral ischemia, as mentioned previously. Animals received systemic delivery of PBS (control, $n = 11$), NPC-EVs low (EVs equivalent to 2×10^5 NPCs, $n = 12$), NPC-EVs medium (EVs equivalent to 2×10^6 NPCs, $n = 11$), or NPC-EVs high (EVs equivalent to 2×10^7 NPCs, $n = 12$), MSC-EVs low (EVs equivalent to 2×10^5 MSCs, $n = 12$), MSC-EVs medium (EVs equivalent to 2×10^6 MSCs, $n = 12$), or MSC-EVs high (EVs equivalent to 2×10^7 MSCs, $n = 13$) 24 h, 72 h, and 120 h post-stroke. The first injections at 24 h were done via cannulation of the right femoral vein, whereas the following injections used a retroorbital injection delivery. On day 70 after stroke induction,

biotinylated dextran amine (BDA) was injected using a Hamilton syringe at 0.5 mm rostral from bregma, 2.5 mm lateral from bregma, and 1.5 mm ventral from the cortical surface. Axonal density was measured 84 days post-stroke, i.e., 14 days after injection of BDA. There was a significant difference in the EV medium and EV high dosage (NPC-EVs only) groups compared with the control group ($p = 0.0049$ in NPC-EV medium group, $p = 0.0331$ in NPC-EV high group, $p = 0.0075$ in MSC-EV medium group). Scale bars, 200 μm . Asterisk indicates significant difference from control with $p < 0.05$. EV, extracellular vesicles; MSC, mesenchymal stem cells; NPC, neural progenitor cell; PBS, phosphate-buffered saline

respect, precipitation methods using PEG or others offer quick and easy handling of large cell supernatant volumes for EV enrichment, although none of these techniques currently qualify for EV enrichment under GMP standards. Previous work from our own group systematically analyzed the PEG precipitation approach in direct comparison with standard EV enrichment procedures on HEK293T cells [33]. The latter revealed the PEG approach to be not inferior to standard EV enrichment procedures using HEK293T cells. Compared with the ultracentrifugation method, the PEG method can concentrate a high volume of conditioned medium in low centrifugation force (4500g) which can reduce EV damage from shear force during the ultracentrifugation process. Although basic EV properties such as the size should be unaffected when dealing with different cell sources [53], the optimal concentrations of these cell sources under different isolation methods remains a matter of debate. To the best of our knowledge, PEG precipitation has not been used for the enrichment of SVZ-derived NPC-EVs. In order to exclude an impact of PEG precipitation on NPC-derived EVs, a detailed characterization of the latter was therefore performed.

Using PEG 6000, we successfully isolated EVs from NPC-conditioned medium. The purification rates obtained by this method were high for NPC-EVs, as indicated in the mass spectrometric analysis result. Especially, EV negative markers such as APOA1, UMOD, and ALB were close to the detection threshold or not detectable at all in our PEG method group and ultracentrifugation only group. Likewise, the distribution patterns were similar to

EVs enriched with ultracentrifugation only, which is still regarded as a gold standard [19]. Our observations are in line with previous work from our group on the comparison of the PEG method and direct ultracentrifugation or differential centrifugation, indicating that PEG does not significantly affect the purity of EVs [33], although artifacts and aggregations still occur as observed in the TEM analysis. As a matter of fact, previous studies on EV application under pathological conditions such as Alzheimer's disease [54] and stroke [55], have either focused on exosomes only or used the general term of EVs, which might be more convenient in light of a therapeutic approach. The mass spectrometric analyses on NPC-EVs as performed in the present work indicated expression patterns of both exosomal markers and microvesicle markers [19]. Some of these proteins found in our EV samples are well-known key mediators of neuroprotection and neurogenesis. The heat shock protein HSP70, for instance, was highly abundant in NPC-derived EVs. HSP70 has frequently been described to mediate a plethora of signaling cascades, all of which contribute to an enhanced resistance of neural cells under hostile hypoxic or ischemic conditions [56]. Under such circumstances, HSP70 has been shown to modify oxidative stress and proteasomal activity of cerebral tissue exposed to hypoxic or ischemic injury, resulting in enhanced cell survival and increased neurological recovery of stroke rodents [56]. The increased resistance of cerebral organoids exposed to OGD injury treated with NPC-EVs might, therefore,

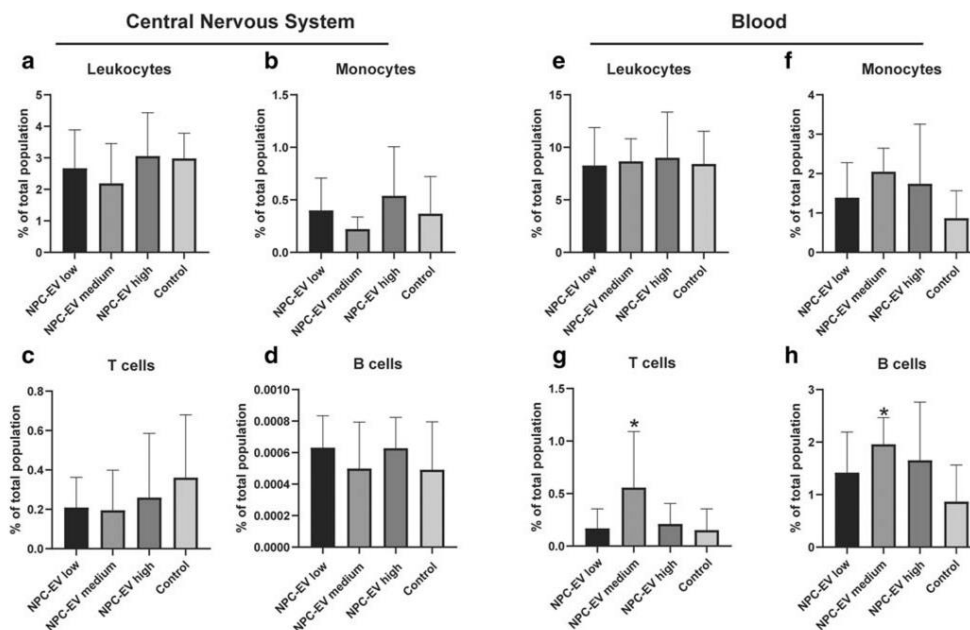


Fig. 7 NPC-EVs reverse post-ischemic peripheral immunosuppression at 7 days after ischemia. Mice were subjected to cerebral ischemia for 60 min followed by reperfusion for 7 days. The animals ($n = 5$ per condition) received systemic delivery of PBS (control), NPC-EVs low (EVs equivalent to 2×10^5 NPCs), NPC-EVs medium (EVs equivalent to 2×10^6 NPCs), or NPC-EVs high (EVs equivalent to 2×10^7 NPCs) 24 h, 72 h, and 120 h post-stroke. Flow cytometry was analyzed with FlowJo software. **a–d** show the quantitative analysis from CNS samples for a

CD45⁺ int⁻, **b** CD11b⁺, **c** CD3⁺, and **d** CD19⁺ cells. In **e–h**, the quantitative analyses from blood samples for **e** CD45⁺ int⁻, **f** CD11b⁺, **g** CD3⁺, and **h** CD19⁺ cells are given. NPC-EV medium increased both T cell ($p = 0.0014$) and B cell populations ($p = 0.0015$) in the peripheral blood but did not affect the CNS. All data are given as means \pm S.D.. Asterisk indicates significant difference from control, $p < 0.05$. CNS, central nervous system; EV, extracellular vesicles; NPC, neural progenitor cell

be at least partially mediated by proteins such as HSP70 and others.

Since pluripotent stem cell-derived NSC-EVs have recently been proven to increase tissue rescue and functional outcomes in translational murine and porcine stroke models [49, 50], our data support the hypothesis that EVs from different cell sources including SVZ-derived NPCs could induce neurological recovery as well. As indicated before, EVs do not only carry diverse sets of proteins but also contain DNA and non-coding RNA, among which are miRNAs of particular interest. The latter has been extensively studied under physiological and pathological conditions alike, not only related to cerebral ischemia where they serve both as biomarkers and therapeutic tools [57]. Screening for selected miRNAs to be likely expressed in NPC-derived EVs revealed enhanced levels of miR-124, which is among the most abundant miRNAs in the adult mammalian brain [58, 59]. miR-124 affects a plethora of signaling molecules such as the recently identified inhibition of deubiquitination of Usp14, significantly contributing to the reduction of post-stroke brain injury in

rodents [60]. Increased levels of miR-124 and others such as the microRNA 17-92 cluster found in NPC-EVs, known to contribute to neuroprotection or enhanced neuroregeneration [61–67], might thus further enhance the resistance of cells and tissues against hypoxia or ischemia. Since EVs are able to transfer cargo-like miRNAs to target cells [68], it is fair enough to hypothesize that NPC-EVs yield protection of cerebral organoids and brain tissue using this way of action. In this context, recent research has demonstrated that oligodendrocytes are able to transfer mitochondria toward neurons via microvesicles upon induction of hypoxia, a mechanism that might also be of relevance under the conditions chosen for the present work [69–71]. Elucidating such a precise mechanism was, however, beyond the scope of the present work which set emphasis on the therapeutic potential of NPC-EVs rather than on mechanisms involved in such a process.

The therapeutic potential of stem cells and the different mechanisms being involved greatly depend on delivery routes and transplantation timing [3]. Indeed, systemic delivery of MSCs or NPCs under experimental stroke conditions reduces

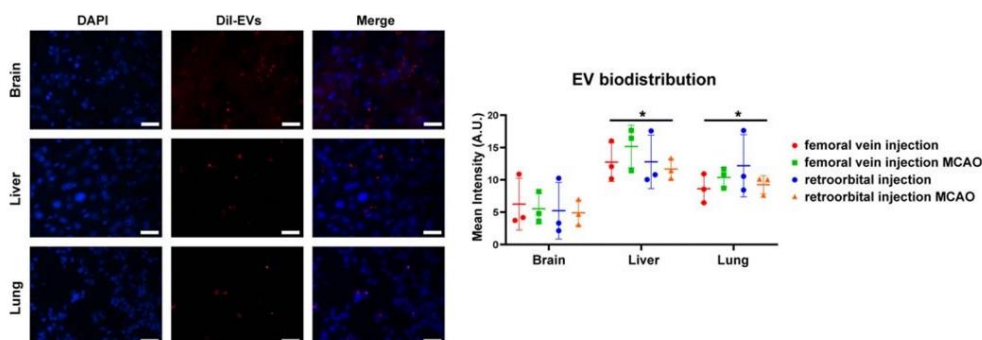


Fig. 8 Biodistribution patterns of NPC-EVs in vivo. Representative immunofluorescence images displaying the biodistribution of EVs in various organs under different delivery routes and conditions (femoral vein injection, femoral vein injection after MCAO, retroorbital injection, and retroorbital injection after MCAO). The organs selected for qualitative and quantitative analysis included the brain, liver, and lung (red color shows the Dil marker for EV detection). Most EVs were found in the liver ($p=0.0023$ compared with the brain) and in the lung ($p=0.0035$ compared with the brain). However, the NPC-EV biodistribution patterns

were of no difference between the liver and the lung. Different delivery routes and conditions also did not affect the biodistribution of NPC-EVs in peripheral organs. The representative photographs refer to mice exposed to MCAO followed by femoral vein injection of EVs. Scale bars, 200 μm . Data are shown as mean \pm S.D.; asterisk indicates significant difference from the brain, $p < 0.05$, $n = 3$ animals per group. EVs, extracellular vesicles; MCAO, middle cerebral artery occlusion; NPC, neural progenitor cell

post-stroke brain injury, enhances neurological recovery, and stimulates neuroregenerative processes [3, 72, 73]. Systemic delivery of MSC-derived EVs, likewise, mediates the aforementioned effects in a similar fashion [17]. Both timing and the delivery route were chosen following a previously established protocol for the intravenous application of MSC-derived EVs [17], although future studies might enhance the therapeutic time frame for EVs even further. Contrary to grafted stem cells, which predominantly do not reach the brain and which involve possible side effects such as neoplasia [74], EVs pass the blood-brain barrier [75]. Recent work has demonstrated that systemic injection of exosomes results in intracerebral enrichment of siRNA derived from these ectopic exosomes [76]. Consequently, the systemic injection of NPC-derived EVs is likely to induce neurological recovery and promote neuroregeneration via enrichment of both cargo proteins and non-coding RNAs after passing of the blood-brain barrier by ectopic EVs. Interestingly, NPC-EVs did not affect post-stroke central immune responses, which is in line with our data acquired on the application of MSC-EVs. Rather, NPC-EVs reverse the post-stroke immunosuppression, as was observed for MSC-EVs. In detail, NPC-EVs increased both peripheral T and B cell numbers, with the latter being known to support neurogenesis and functional recovery after stroke [77]. The idea of a peripheral way of action of systemically delivered NPC-EVs is further backed up by the fact that labeled NPC-EVs predominantly end up in peripheral organs such as the lung and the liver rather than in the brain. However, additional studies regarding homing and targeting of ectopic EVs are required to elucidate these underlying mechanisms further.

In our study, medium dosages of NPC-EVs (and also MSC-EVs) showed optimal outcomes when compared with either low or high dosages of EVs. Although we do not have clear evidence, it appears to be feasible that high dosages might lead to the formation of embolisms, resulting in the early death of animals. On the contrary, low dosages of EVs might result in an insufficient concentration of either cargo proteins or non-coding RNAs, thus failing to induce neuroprotection or neuroregeneration. However, the medium dosages of NPC-EVs and MSC-EVs only showed transiently beneficial effects in the balance beam test, which might be due to the lower sensitivity of the balance beam test when compared with the tight rope test and the corner turn test at later stages of the disease [78, 79]. As such, high sensitivity is of utmost importance, especially at chronic stages of the disease. Studies on the dose-dependent effects of EVs are surprisingly short, but Tabak et al. indeed suggest that EVs affect target tissues in a dose-dependent manner [80]. Thus, the present work also indicates that future studies should pay attention to the EV dosage chosen when planning both pre-clinical investigations and clinical trials.

In conclusion, the present study demonstrates that SVZ-derived NPC-EVs are effective as therapeutic tools under experimental stroke conditions. The underlying mechanisms appear to be pleiotropic and complex but are in part due to a modulation of peripheral post-stroke immune responses. In light of NPC-EVs being non-inferior to MSC-EVs, the idea of EVs as general therapeutic tools independent of cell sources is thus further supported. As a matter of fact, the tremendous translational potential of EVs is evident, with distinct advantages when compared with stem cell transplantation. After a

myriad of negative clinical trials in the field of neuroprotective drugs against stroke, EVs might revolutionize modern stroke treatment as an available tool next to clinically established re-canalization strategies.

Acknowledgments Open Access funding provided by Projekt DEAL. We thank Irina Graf and Regine Kruse (both Goettingen, Germany) for excellent technical assistance. We also thank Dr. Sarah K. Williams (Heidelberg, Germany) for proofreading of the manuscript.

Authors' Contributions - Research and experiments were performed by Zheng, Zhang, Kuang, Venkataramani, Jin, Zafeiriou, Lenz, Moebius, Weber, and Doepfner.

- Design and concept of the study were from Zheng and Doepfner.
- Zheng, Doepfner, Hein, Hemmann, Urlaub, Bähr, and Zimmermann wrote the manuscript.
- Financial support was provided by Bähr, Doepfner, and Zimmermann.

Funding Information This study was funded by TÜBITAK (to T.R.D.). P.M.Z. is funded by the Deutsche Forschungsgemeinschaft (DFG, German Research Foundation) under Germany's Excellence Strategy—EXC 2067/1-390729940. W.H.Z. is supported by the DFG (ZI 708/10-1; CRC 1002 C04 and S01; IRTG1816 RP12; EXC 2067/1-390729940), by the German Center for Cardiovascular Research (DZHK), and the Fondation Leducq (14CVD04).

Compliance with Ethical Standards

Conflict of Interest The authors declare that they have no conflict of interest.

Ethical Approval This article does not contain any studies with human participants performed by any of the authors. All animal experiments were performed with governmental approval according to the NIH guidelines for the care and use of laboratory animals. Both the STAIR criteria and the ARRIVE guidelines have been followed.

Open Access This article is licensed under a Creative Commons Attribution 4.0 International License, which permits use, sharing, adaptation, distribution and reproduction in any medium or format, as long as you give appropriate credit to the original author(s) and the source, provide a link to the Creative Commons licence, and indicate if changes were made. The images or other third party material in this article are included in the article's Creative Commons licence, unless indicated otherwise in a credit line to the material. If material is not included in the article's Creative Commons licence and your intended use is not permitted by statutory regulation or exceeds the permitted use, you will need to obtain permission directly from the copyright holder. To view a copy of this licence, visit <http://creativecommons.org/licenses/by/4.0/>.

References

- Bacigaluppi M, Pluchino S, Peruzzotti-Jametti L, Kilic E, Kilic U, Salani G, et al. Delayed post-ischaemic neuroprotection following systemic neural stem cell transplantation involves multiple mechanisms. *Brain*. 2009;132(Pt 8):2239–51.
- Banerjee S, Williamson DA, Habib N, Chataway J. The potential benefit of stem cell therapy after stroke: an update. *Vasc Health Risk Manag*. 2012;8:569–80.
- Doepfner TR, et al. Effects of acute versus post-acute systemic delivery of neural progenitor cells on neurological recovery and brain remodeling after focal cerebral ischemia in mice. *Cell Death Dis*. 2014;5:e1386.
- Shen LH, Li Y, Chen J, Zhang J, Vanguri P, Borneman J, et al. Intracarotid transplantation of bone marrow stromal cells increases axon-myelin remodeling after stroke. *Neuroscience*. 2006;137(2):393–9.
- Ukai R, Honmou O, Harada K, Houkin K, Hamada H, Kocsis JD. Mesenchymal stem cells derived from peripheral blood protects against ischemia. *J Neurotrauma*. 2007;24(3):508–20.
- Doepfner TR, Ewert TA, Tönges L, Herz J, Zechariah A, ElAli A, et al. Transduction of neural precursor cells with TAT-heat shock protein 70 chaperone: therapeutic potential against ischemic stroke after intrastriatal and systemic transplantation. *Stem Cells*. 2012;30(6):1297–310.
- Lee RH, Pulin AA, Seo MJ, Kota DJ, Ylostalo J, Larson BL, et al. Intravenous hMSCs improve myocardial infarction in mice because cells embolized in lung are activated to secrete the anti-inflammatory protein TSG-6. *Cell Stem Cell*. 2009;5(1):54–63.
- Darsalia V, Kallur T, Kokaia Z. Survival, migration and neuronal differentiation of human fetal striatal and cortical neural stem cells grafted in stroke-damaged rat striatum. *Eur J Neurosci*. 2007;26(3):605–14.
- Wei L, Cui L, Snider BJ, Rivkin M, Yu SS, Lee CS, et al. Transplantation of embryonic stem cells overexpressing Bcl-2 promotes functional recovery after transient cerebral ischemia. *Neurobiol Dis*. 2005;19(1–2):183–93.
- McDonald JW, et al. Transplanted embryonic stem cells survive, differentiate and promote recovery in injured rat spinal cord. *Nat Med*. 1999;5(12):1410–2.
- Zawada WM, Zastrow DJ, Clarkson ED, Adams FS, Bell KP, Freed CR. Growth factors improve immediate survival of embryonic dopamine neurons after transplantation into rats. *Brain Res*. 1998;786(1–2):96–103.
- Hao P, Liang Z, Piao H, Ji X, Wang Y, Liu Y, et al. Conditioned medium of human adipose-derived mesenchymal stem cells mediates protection in neurons following glutamate excitotoxicity by regulating energy metabolism and GAP-43 expression. *Metab Brain Dis*. 2014;29(1):193–205.
- Timmers L, Lim SK, Arslan F, Armstrong JS, Hoefler IE, Doevendans PA, et al. Reduction of myocardial infarct size by human mesenchymal stem cell conditioned medium. *Stem Cell Res*. 2007;1(2):129–37.
- Hsieh JY, Wang HW, Chang SJ, Liao KH, Lee IH, Lin WS, et al. Mesenchymal stem cells from human umbilical cord express preferentially secreted factors related to neuroprotection, neurogenesis, and angiogenesis. *PLoS One*. 2013;8(8):e72604.
- Scheibe F, Klein O, Klose J, Priller J. Mesenchymal stromal cells rescue cortical neurons from apoptotic cell death in an in vitro model of cerebral ischemia. *Cell Mol Neurobiol*. 2012;32(4):567–76.
- Tate CC, Fonck C, McGrogan M, Case CC. Human mesenchymal stromal cells and their derivative, SB623 cells, rescue neural cells via trophic support following in vitro ischemia. *Cell Transplant*. 2010;19(8):973–84.
- Doepfner TR, Herz J, Görgens A, Schlechter J, Ludwig AK, Radtke S, et al. Extracellular vesicles improve post-stroke neuroregeneration and prevent postischemic immunosuppression. *Stem Cells Transl Med*. 2015;4(10):1131–43.
- Yang Y, Cai Y, Zhang Y, Liu J, Xu Z. Exosomes secreted by adipose-derived stem cells contribute to angiogenesis of brain microvascular endothelial cells following oxygen-glucose deprivation in vitro through microRNA-181b/TRPM7 Axis. *J Mol Neurosci*. 2018;65(1):74–83.
- Thery C, et al. Minimal information for studies of extracellular vesicles 2018 (MISEV2018): a position statement of the

- International Society for Extracellular Vesicles and update of the MISEV2014 guidelines. *J Extracell Vesicles*. 2018;7(1):1535750.
20. Kim DK, et al. EVpedia: an integrated database of high-throughput data for systemic analyses of extracellular vesicles. *J Extracell Vesicles*. 2013;2.
 21. Mathivanan S, Fahner CJ, Reid GE, Simpson RJ. ExoCarta 2012: database of exosomal proteins, RNA and lipids. *Nucleic Acids Res*. 2012;40(Database issue):D1241–4.
 22. Doyle LM, Wang MZ. Overview of extracellular vesicles, their origin, composition, purpose, and methods for exosome isolation and analysis. *Cells*. 2019;8(7).
 23. Cantaluppi V, Gatti S, Medica D, Figliolini F, Bruno S, Deregibus MC, et al. Microvesicles derived from endothelial progenitor cells protect the kidney from ischemia-reperfusion injury by microRNA-dependent reprogramming of resident renal cells. *Kidney Int*. 2012;82(4):412–27.
 24. Gatti S, et al. Microvesicles derived from human adult mesenchymal stem cells protect against ischaemia-reperfusion-induced acute and chronic kidney injury. *Nephrol Dial Transplant*. 2011;26(5):1474–83.
 25. Lai RC, Arslan F, Lee MM, Sze NS, Choo A, Chen TS, et al. Exosome secreted by MSC reduces myocardial ischemia/reperfusion injury. *Stem Cell Res*. 2010;4(3):214–22.
 26. Li T, Yan Y, Wang B, Qian H, Zhang X, Shen L, et al. Exosomes derived from human umbilical cord mesenchymal stem cells alleviate liver fibrosis. *Stem Cells Dev*. 2013;22(6):845–54.
 27. Xin H, Li Y, Cui Y, Yang JJ, Zhang ZG, Chopp M. Systemic administration of exosomes released from mesenchymal stromal cells promote functional recovery and neurovascular plasticity after stroke in rats. *J Cereb Blood Flow Metab*. 2013;33(11):1711–5.
 28. Joerger-Messerli MS, et al. Extracellular vesicles derived from Wharton's jelly mesenchymal stem cells prevent and resolve programmed cell death mediated by perinatal hypoxia-ischemia in neuronal cells. *Cell Transplant*. 2018;27(1):168–80.
 29. Ophelders DR, Wolfs TG, Jellema RK, Zwanenburg A, Andriessen P, Delhaas T, et al. Mesenchymal stromal cell-derived extracellular vesicles protect the fetal brain after hypoxia-ischemia. *Stem Cells Transl Med*. 2016;5(6):754–63.
 30. Rumajogee P, et al. Exogenous neural precursor cell transplantation results in structural and functional recovery in a hypoxic-ischemic hemiplegic mouse model. *eNeuro*. 2018;5(5).
 31. Wilcox JT, Satkunendarajah K, Zuccato JA, Nassiri F, Fehlings MG. Neural precursor cell transplantation enhances functional recovery and reduces astrogliosis in bilateral compressive/contusive cervical spinal cord injury. *Stem Cells Transl Med*. 2014;3(10):1148–59.
 32. Zhang P, Li J, Liu Y, Chen X, Lu H, Kang Q, et al. Human embryonic neural stem cell transplantation increases subventricular zone cell proliferation and promotes peri-infarct angiogenesis after focal cerebral ischemia. *Neuropathology*. 2011;31(4):384–91.
 33. Ludwig AK, de Miroschedji K, Doepfner TR, Börger V, Ruesing J, Rebmann V, et al. Precipitation with polyethylene glycol followed by washing and pelleting by ultracentrifugation enriches extracellular vesicles from tissue culture supernatants in small and large scales. *J Extracell Vesicles*. 2018;7(1):1528109.
 34. Sokolova V, Ludwig AK, Homung S, Rotan O, Hom PA, Epple M, et al. Characterisation of exosomes derived from human cells by nanoparticle tracking analysis and scanning electron microscopy. *Colloids Surf B Biointerfaces*. 2011;87(1):146–50.
 35. Peters PJ, Pierson J. Immunogold labeling of thawed cryosections. *Methods Cell Biol*. 2008;88:131–49.
 36. Atanasov I, Urlaub H. Increased proteome coverage by combining PAGE and peptide isoelectric focusing: comparative study of gel-based separation approaches. *Proteomics*. 2013;13(20):2947–55.
 37. Chen SR, Cai WP, Dai XJ, Guo AS, Chen HP, Lin GS, et al. Research on miR-126 in glioma targeted regulation of PTEN/PI3K/Akt and MDM2-p53 pathways. *Eur Rev Med Pharmacol Sci*. 2019;23(8):3461–70.
 38. Yao L, Zhu Z, Wu J, Zhang Y, Zhang H, Sun X, et al. MicroRNA-124 regulates the expression of p62/p38 and promotes autophagy in the inflammatory pathogenesis of Parkinson's disease. *FASEB J*. 2019;33(7):8648–65.
 39. Zheng L, et al. Overexpression of microRNA-145 ameliorates astrocyte injury by targeting aquaporin 4 in cerebral ischemic stroke. *Biomed Res Int*. 2017;2017:9530951.
 40. Huang B, Jiang XC, Zhang TY, Hu YL, Tabata Y, Chen Z, et al. Peptide modified mesenchymal stem cells as targeting delivery system transfected with miR-133b for the treatment of cerebral ischemia. *Int J Pharm*. 2017;531(1):90–100.
 41. Xin H, Katakowski M, Wang F, Qian JY, Liu XS, Ali MM, et al. MicroRNA cluster miR-17-92 cluster in exosomes enhance neuroplasticity and functional recovery after stroke in rats. *Stroke*. 2017;48(3):747–53.
 42. Tiburcy M, Hudson JE, Balfanz P, Schlick S, Meyer T, Chang Liao ML, et al. Defined engineered human myocardium with advanced maturation for applications in heart failure modeling and repair. *Circulation*. 2017;135(19):1832–47.
 43. Balkaya M, Kröber JM, Rex A, Endres M. Assessing post-stroke behavior in mouse models of focal ischemia. *J Cereb Blood Flow Metab*. 2013;33(3):330–8.
 44. Mirzaei H, Momeni F, Saadatpour L, Sahebkar A, Goodarzi M, Masoudifar A, et al. MicroRNA: relevance to stroke diagnosis, prognosis, and therapy. *J Cell Physiol*. 2018;233(2):856–65.
 45. Xing C, Arai K, Lo EH, Hommel M. Pathophysiologic cascades in ischemic stroke. *Int J Stroke*. 2012;7(5):378–85.
 46. Eggenhofer E, et al. The life and fate of mesenchymal stem cells. *Front Immunol*. 2014;5:148.
 47. Zagrean AM, et al. Multicellular crosstalk between exosomes and the neurovascular unit after cerebral ischemia. Therapeutic implications. *Front Neurosci*. 2018;12:811.
 48. Park KS, Bandeira E, Shelke GV, Lässer C, Lötvall J. Enhancement of therapeutic potential of mesenchymal stem cell-derived extracellular vesicles. *Stem Cell Res Ther*. 2019;10(1):288.
 49. Webb RL, et al. Human neural stem cell extracellular vesicles improve recovery in a porcine model of ischemic stroke. *Stroke*. 2018;49(5):1248–56.
 50. Webb RL, Kaiser EE, Scoville SL, Thompson TA, Fatima S, Pandya C, et al. Human neural stem cell extracellular vesicles improve tissue and functional recovery in the murine thromboembolic stroke model. *Transl Stroke Res*. 2018;9(5):530–9.
 51. Yamashita T, Ninomiya M, Hernández Acosta P, García-Vertugo JM, Sunabori T, Sakaguchi M, et al. Subventricular zone-derived neuroblasts migrate and differentiate into mature neurons in the post-stroke adult striatum. *J Neurosci*. 2006;26(24):6627–36.
 52. Lane RE, Korb D, Trau M, Hill MM. Purification protocols for extracellular vesicles. *Methods Mol Biol*. 2017;1660:111–30.
 53. Haraszti RA, et al. High-resolution proteomic and lipidomic analysis of exosomes and microvesicles from different cell sources. *J Extracell Vesicles*. 2016;5:32570.
 54. Reza-Zaldivar EE, Hernández-Sapiéns MA, Gutiérrez-Mercado YK, Sandoval-Ávila S, Gomez-Pinedo U, Márquez-Aguirre AL, et al. Mesenchymal stem cell-derived exosomes promote neurogenesis and cognitive function recovery in a mouse model of Alzheimer's disease. *Neural Regen Res*. 2019;14(9):1626–34.
 55. Geng W, Tang H, Luo S, Lv Y, Liang D, Kang X, et al. Exosomes from miRNA-126-modified ADSCs promotes functional recovery after stroke in rats by improving neurogenesis and suppressing microglia activation. *Am J Transl Res*. 2019;11(2):780–92.
 56. Kim JY, Han Y, Lee JE, Yenari MA. The 70-kDa heat shock protein (Hsp70) as a therapeutic target for stroke. *Expert Opin Ther Targets*. 2018;22(3):191–9.

57. Bertoli G, Cava C, Castiglioni I. MicroRNAs: new biomarkers for diagnosis, prognosis, therapy prediction and therapeutic tools for breast cancer. *Theranostics*. 2015;5(10):1122–43.
58. Cao X, Pfaff SL, Gage FH. A functional study of miR-124 in the developing neural tube. *Genes Dev*. 2007;21(5):531–6.
59. Mishima T, Mizuguchi Y, Kawahigashi Y, Takizawa T, Takizawa T. RT-PCR-based analysis of microRNA (miR-1 and -124) expression in mouse CNS. *Brain Res*. 2007;1131(1):37–43.
60. Song Y, Li Z, He T, Qu M, Jiang L, Li W, et al. M2 microglia-derived exosomes protect the mouse brain from ischemia-reperfusion injury via exosomal miR-124. *Theranostics*. 2019;9(10):2910–23.
61. Matsuoka H, Tamura A, Kinehara M, Shima A, Uda A, Tahara H, et al. Levels of tight junction protein CLDN1 are regulated by microRNA-124 in the cerebellum of stroke-prone spontaneously hypertensive rats. *Biochem Biophys Res Commun*. 2018;498(4):817–23.
62. Saraiva C, Talhada D, Rai A, Ferreira R, Ferreira L, Bernardino L, et al. MicroRNA-124-loaded nanoparticles increase survival and neuronal differentiation of neural stem cells in vitro but do not contribute to stroke outcome in vivo. *PLoS One*. 2018;13(3):e0193609.
63. Yang J, Zhang X, Chen X, Wang L, Yang G. Exosome mediated delivery of miR-124 promotes neurogenesis after ischemia. *Mol Ther Nucleic Acids*. 2017;7:278–87.
64. Hamzei Taj S, Kho W, Riou A, Wiedermann D, Hoehn M. MiRNA-124 induces neuroprotection and functional improvement after focal cerebral ischemia. *Biomaterials*. 2016;91:151–65.
65. Pan WL, Chopp M, Fan B, Zhang R, Wang X, Hu J, et al. Ablation of the microRNA-17-92 cluster in neural stem cells diminishes adult hippocampal neurogenesis and cognitive function. *FASEB J*. 2019;33(4):5257–67.
66. Jin J, Ko H, Sun T, Kim SN. Distinct function of miR-17-92 cluster in the dorsal and ventral adult hippocampal neurogenesis. *Biochem Biophys Res Commun*. 2018;503(3):1594–8.
67. Yang P, Cai L, Zhang G, Bian Z, Han G. The role of the miR-17-92 cluster in neurogenesis and angiogenesis in the central nervous system of adults. *J Neurosci Res*. 2017;95(8):1574–81.
68. Abels ER, Breakefield XO. Introduction to extracellular vesicles: biogenesis, RNA cargo selection, content, release, and uptake. *Cell Mol Neurobiol*. 2016;36(3):301–12.
69. Frohlich D, et al. Multifaceted effects of oligodendroglial exosomes on neurons: impact on neuronal firing rate, signal transduction and gene regulation. *Philos Trans R Soc Lond Ser B Biol Sci*. 2014;369(1652).
70. Fruhbeis C, et al. Neurotransmitter-triggered transfer of exosomes mediates oligodendrocyte-neuron communication. *PLoS Biol*. 2013;11(7):e1001604.
71. Kramer-Albers EM, et al. Oligodendrocytes secrete exosomes containing major myelin and stress-protective proteins: trophic support for axons? *Proteomics Clin Appl*. 2007;1(11):1446–61.
72. Han Y, et al. Multipotent mesenchymal stromal cell-derived exosomes improve functional recovery after experimental intracerebral hemorrhage in the rat. *J Neurosurg*. 2018;1–11.
73. Mahmood A, Lu D, Chopp M. Marrow stromal cell transplantation after traumatic brain injury promotes cellular proliferation within the brain. *Neurosurgery*. 2004;55(5):1185–93.
74. Erdo F, et al. Host-dependent tumorigenesis of embryonic stem cell transplantation in experimental stroke. *J Cereb Blood Flow Metab*. 2003;23(7):780–5.
75. Matsumoto J, et al. The transport mechanism of extracellular vesicles at the blood-brain barrier. *Curr Pharm Des*. 2017;23(40):6206–14.
76. Alvarez-Erviti L, Seow Y, Yin H, Betts C, Likhani S, Wood MJ. Delivery of siRNA to the mouse brain by systemic injection of targeted exosomes. *Nat Biotechnol*. 2011;29(4):341–5.
77. Ortega SB, et al. B cells migrate into remote brain areas and support neurogenesis and functional recovery after focal stroke in mice. *Proc Natl Acad Sci U S A*. 2020.
78. Schaar KL, Brenneman MM, Savitz SI. Functional assessments in the rodent stroke model. *Exp Transl Stroke Med*. 2010;2(1):13.
79. Zhang L, Schallert T, Zhang ZG, Jiang Q, Amiego P, Li Q, et al. A test for detecting long-term sensorimotor dysfunction in the mouse after focal cerebral ischemia. *J Neurosci Methods*. 2002;117(2):207–14.
80. Tabak S, Schreiber-Avissar S, Beit-Yannai E. Extracellular vesicles have variable dose-dependent effects on cultured draining cells in the eye. *J Cell Mol Med*. 2018;22(3):1992–2000.

Publisher's Note Springer Nature remains neutral with regard to jurisdictional claims in published maps and institutional affiliations.

7 Acknowledgements

This thesis has been written at the Department of Neurology of the University of Göttingen Medical Center (UMG), Germany (director: Prof. Dr. Mathias Bähr). I would like to thank everyone who provided support and encouragement to me through the process of performing the experiments and writing this thesis. However, I would like to especially thank Prof. Dr. Thorsten R. Döppner, M.Sc., for his splendid supervision during all these years. Without him this thesis would have never been possible. Finally, I would also like to express my gratitude to Prof. Dr. Mathias Bähr for giving me the opportunity to work in his department

8 Curriculum Vitae

My name is Xuan Zheng. I was born in the city of Guangzhou in China on February/25/1988. I studied neuroscience at Guangzhou Medical University from 2007 on. After my bachelor degree in 2012, I continued to study neuroscience and received my master of neuroscience degree in 2015. During my master thesis, I found out that most of the stroke patients did not receive rt-PA (recombinant tissue plasminogen activator, an enzyme for thrombolysis) treatment in time, leading to disability and low quality of life. Unfortunately, neuroprotective drugs did not show significant beneficial effects either. The majority of patients recovers very slowly and painfully. A huge number remain constantly disabled and many of them develop respiratory infections, leading to poor prognosis. Since it is not easy to treat stroke patients in time because of the lack of availability of medical resources in China, the recovery rate after stroke is higher in developed countries. Therefore, I started my doctoral thesis under the supervision of Prof. T. R. Döppner in the Department of Neurology at the University Medical Center in Göttingen, Germany, in June 2016. The title of my thesis is "Extracellular vesicles derived from neural progenitor cells stimulate neuroregeneration in a rodent stroke model". Stem cell transplantation and extracellular vesicles have great potential as a potential therapeutic tool in stroke and other diseases, which will hopefully shorten the recovery time for stroke patients. My goal is to use stem cell transplantation and extracellular vesicles to help patients in future clinical applications.